

Exploring the earth with seismic noise: Anthropogenic and exogenic noise sources

Peter Gerstoft, **With help from** Nima Riahi, Mike Bianco,
Slides are available from <http://noiselab.ucsd.edu>

- Noise is full of information.
- Think of characterizing a dark room
- My focus is on extracting information from noise (acoustic, seismic, EM) with the help of signal processing, compressive sensing, and **machine learning**.

Contents:

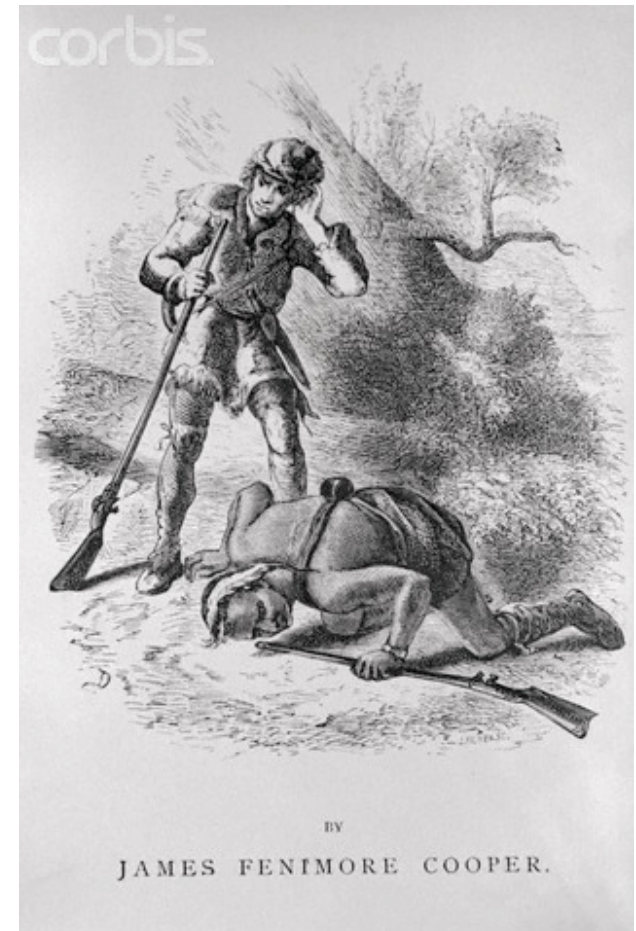
Long Beach array

Observing traffic

Localizing weak sources

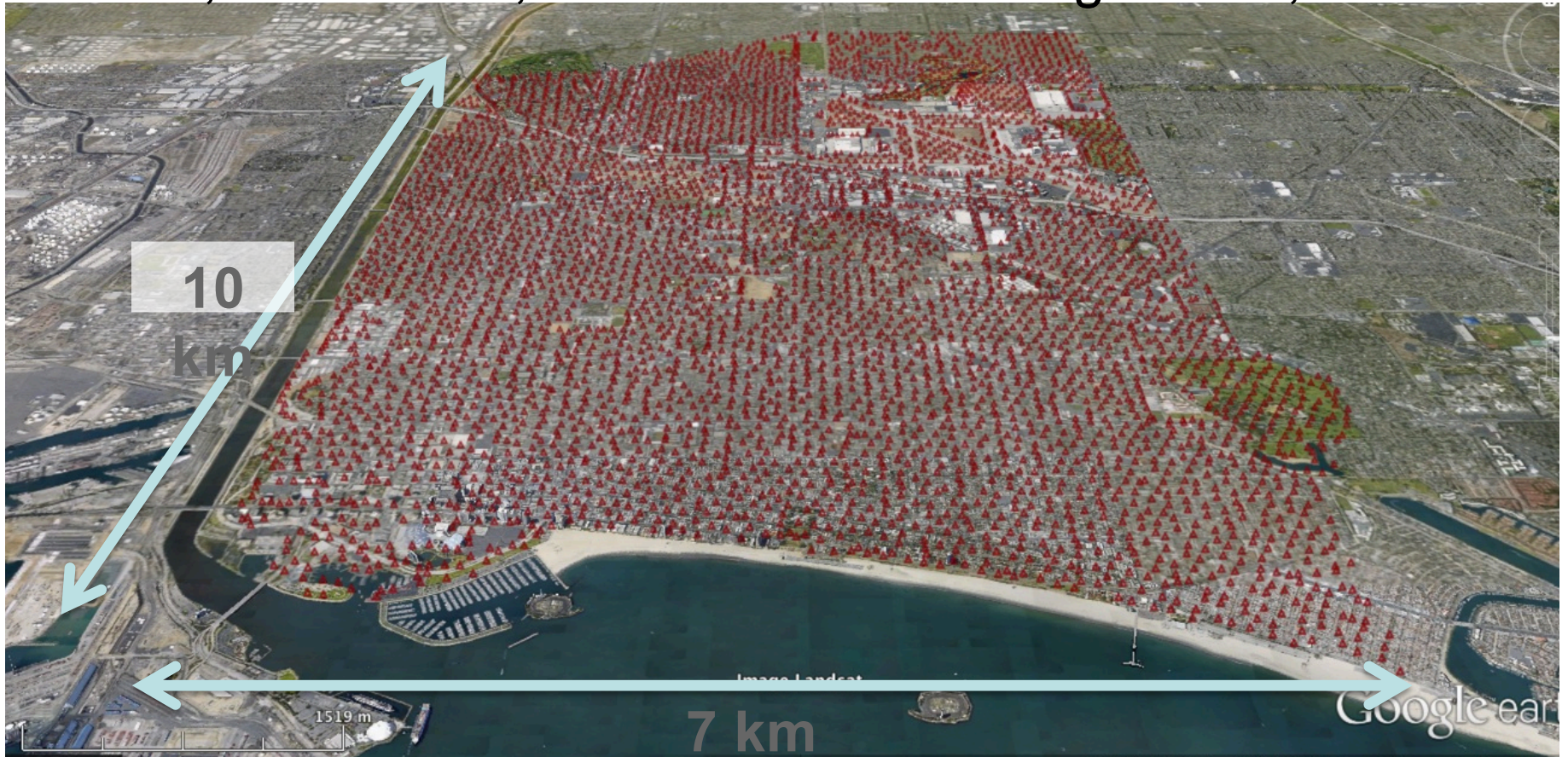
Noise tomography

Antarctica Tsunami generated plate waves



Noise observation on seismic sensor array

March 5—12, 2011: 3TB, 5200 Stations in Long Beach, California



Geophones samples at 250 Hz for 6 months



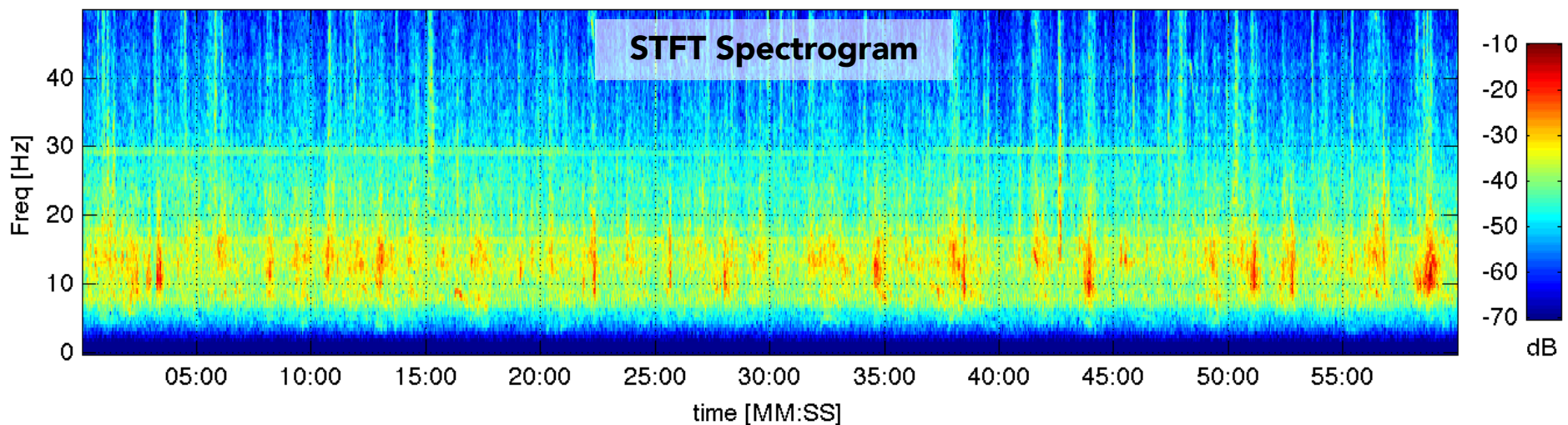
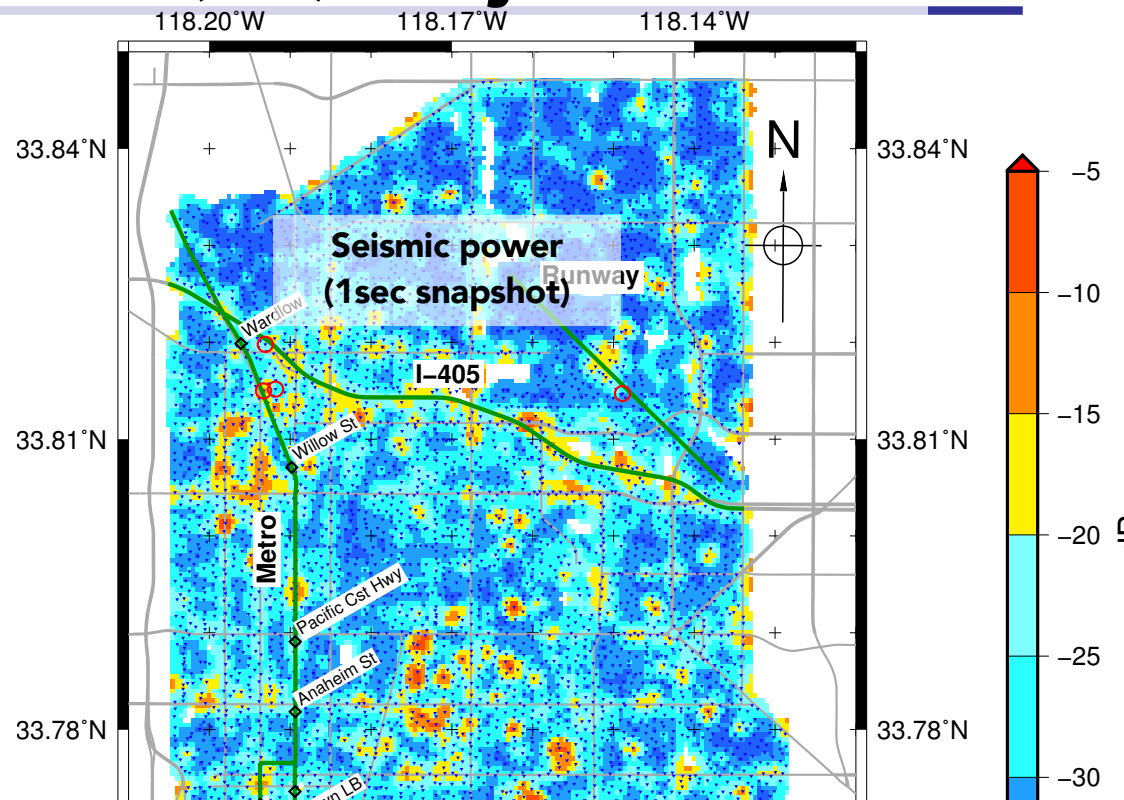
Our motivation: Long Beach (CA) array

Oil industry dataset offers insight into urban noise sources:

- ✓ 5200+ sensors (GPS equipped nodes)
- ✓ Covers 70 km² of urban area
- ✓ Spacing ~100 m
- ✓ 1 week ambient vibrations

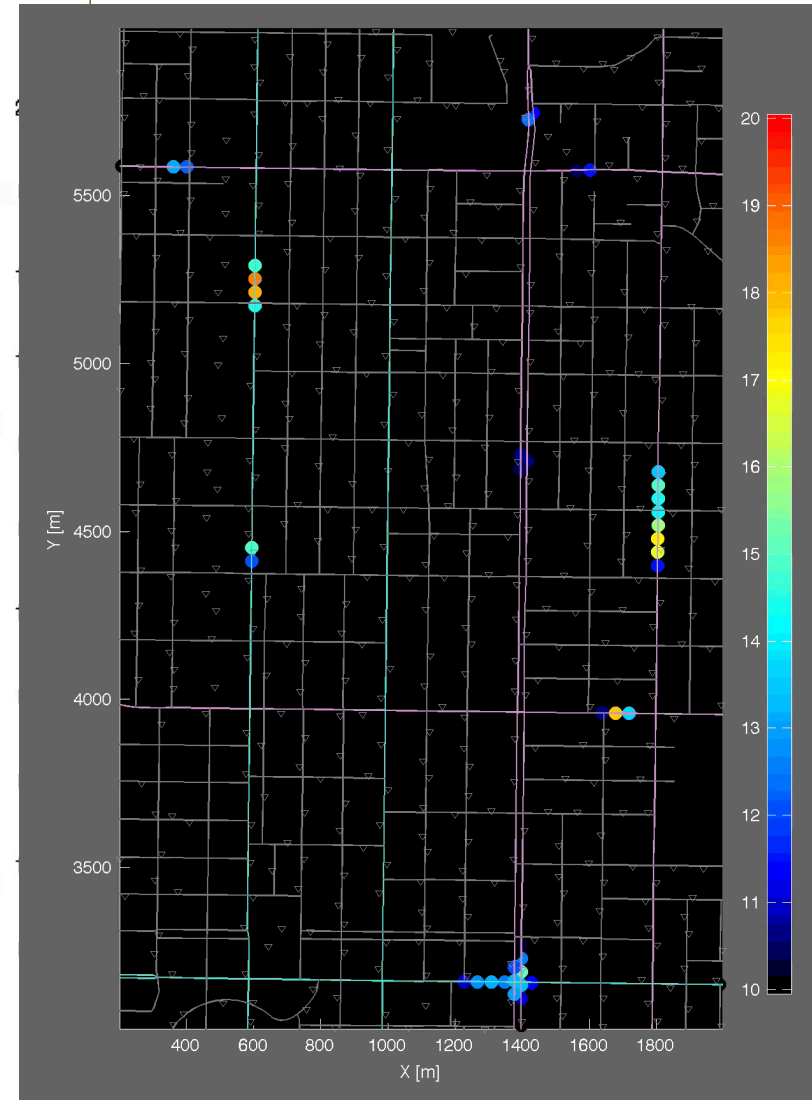
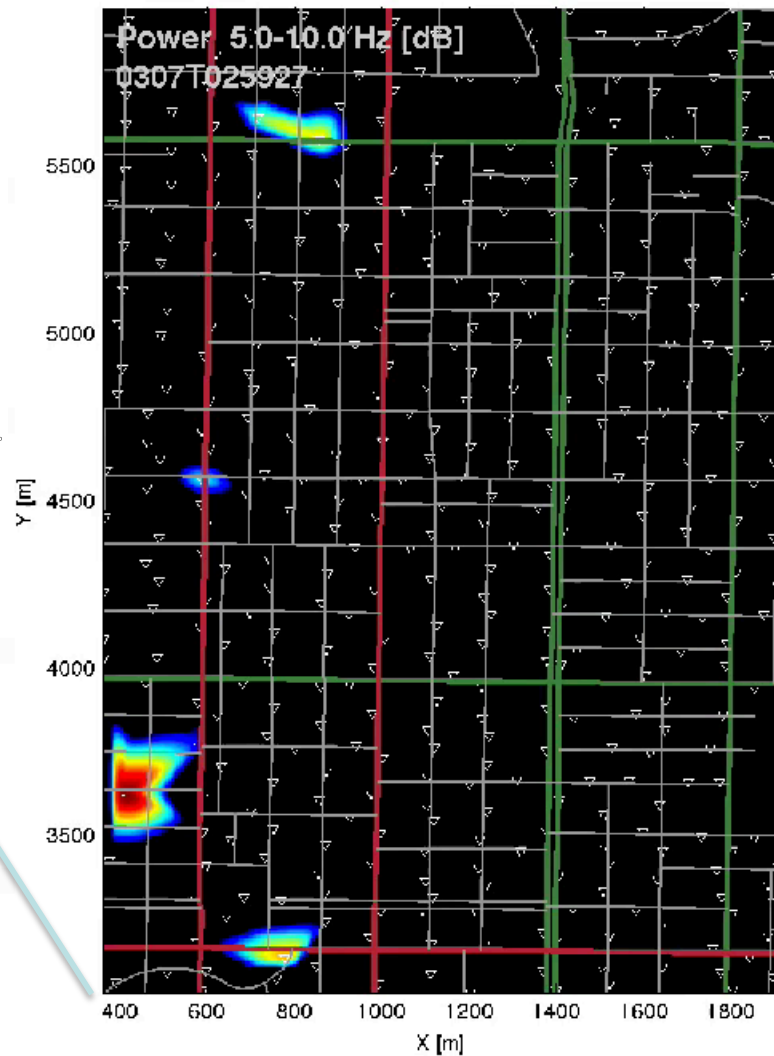
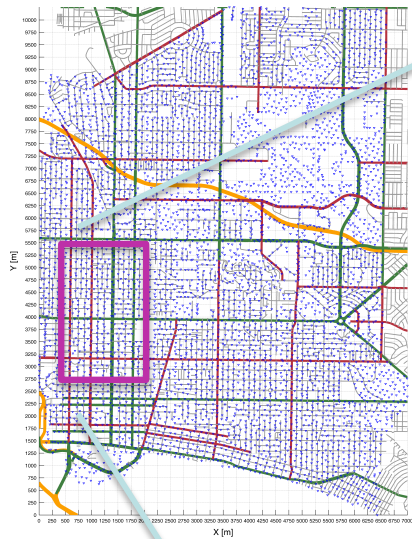
High attenuation in data.

Very limited knowledge about near-surface seismic propagation parameters.



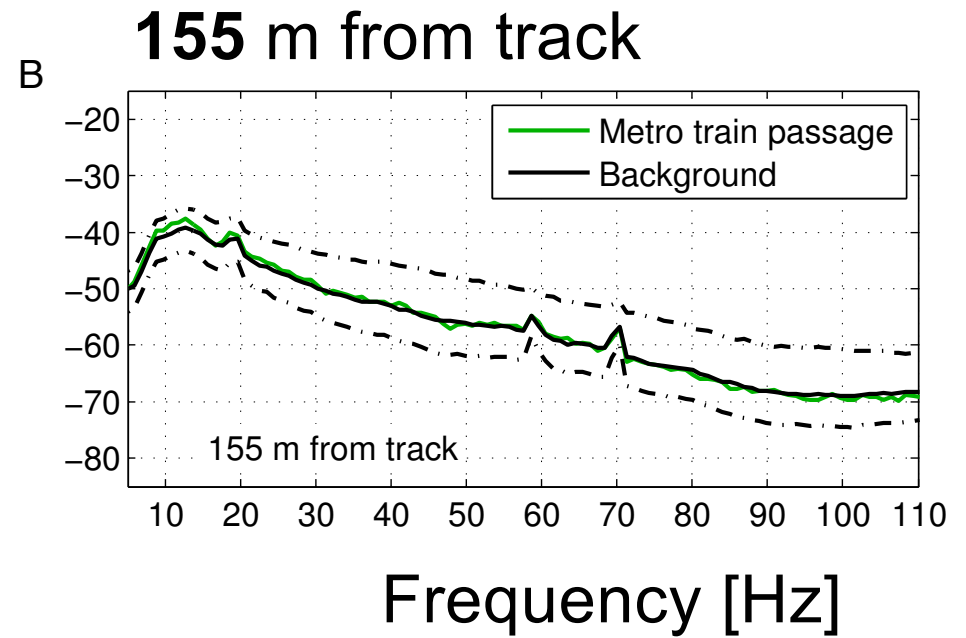
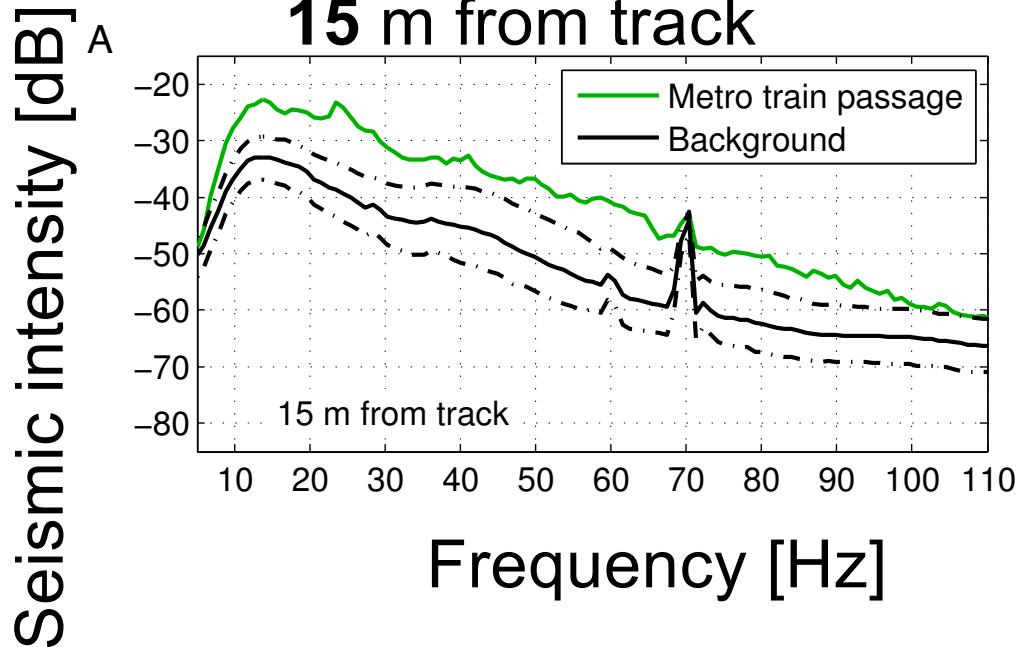
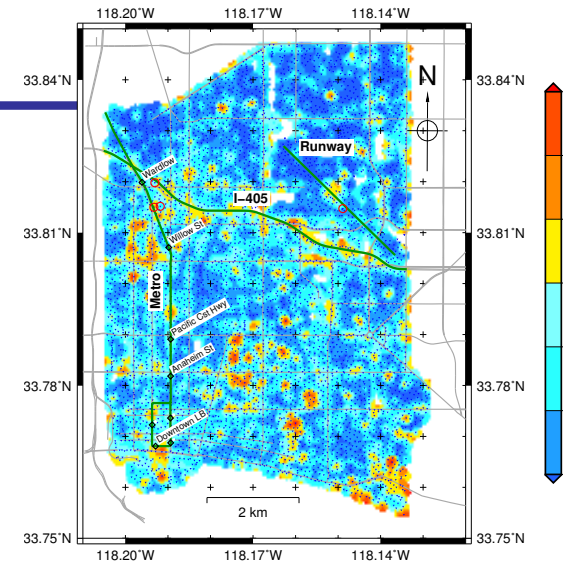
Noise Tracking of Cars/Trains/Airplanes

5200 element Long Beach array (Dan Hollis)

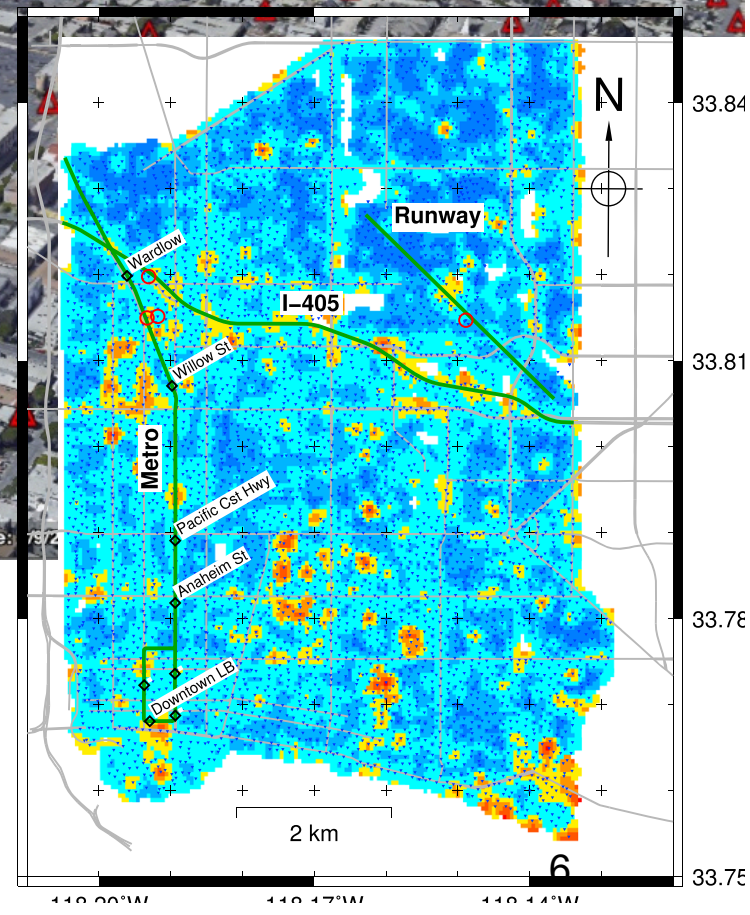
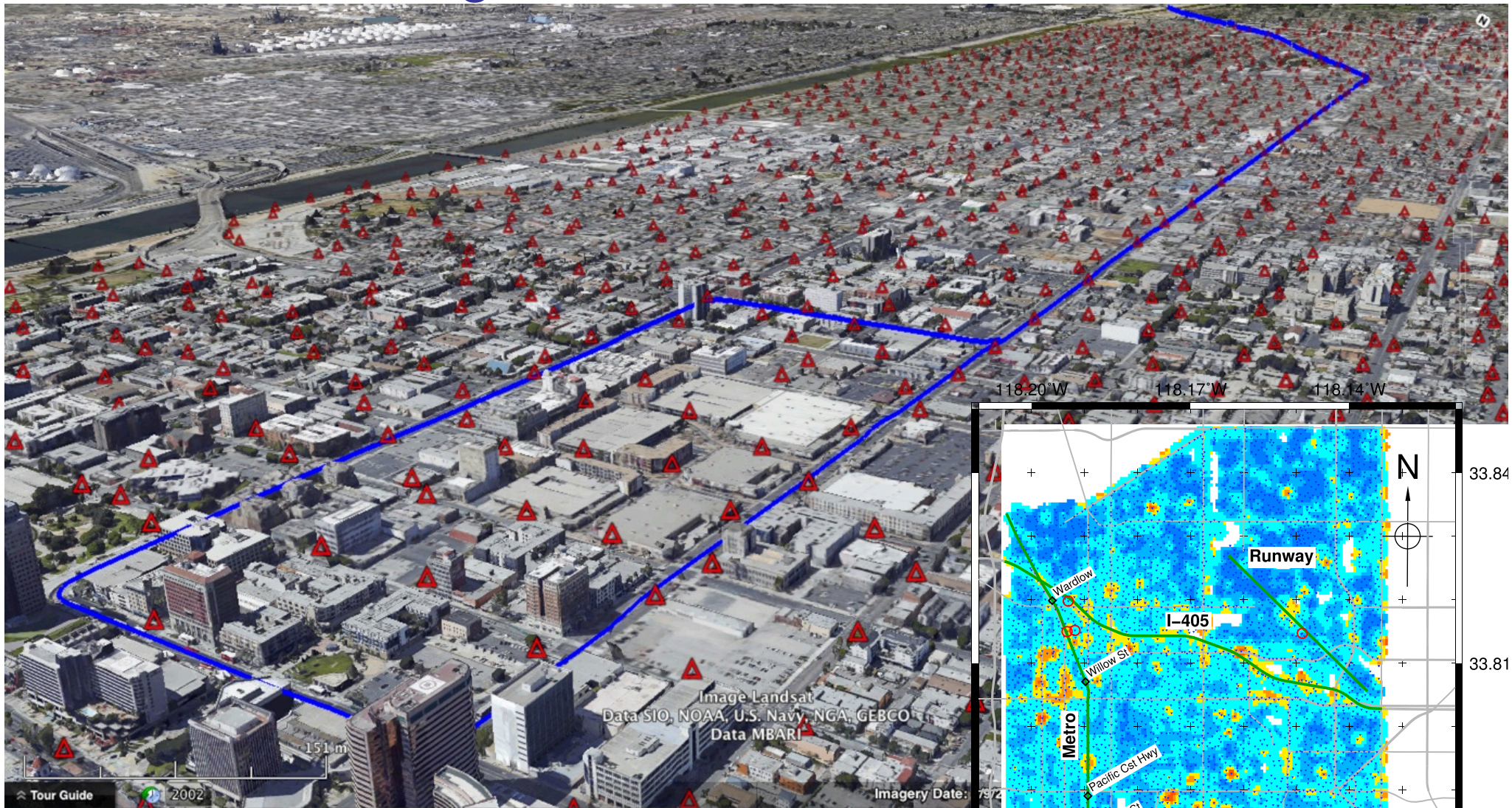


Power spectra

Seismic intensity can be used as source proximity indicator

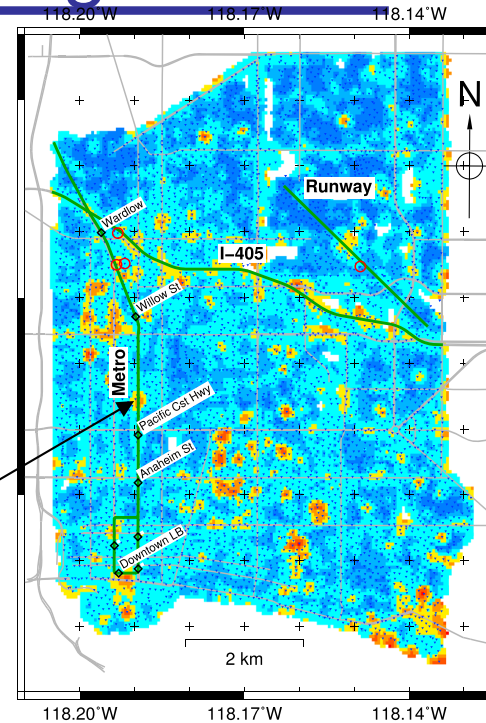
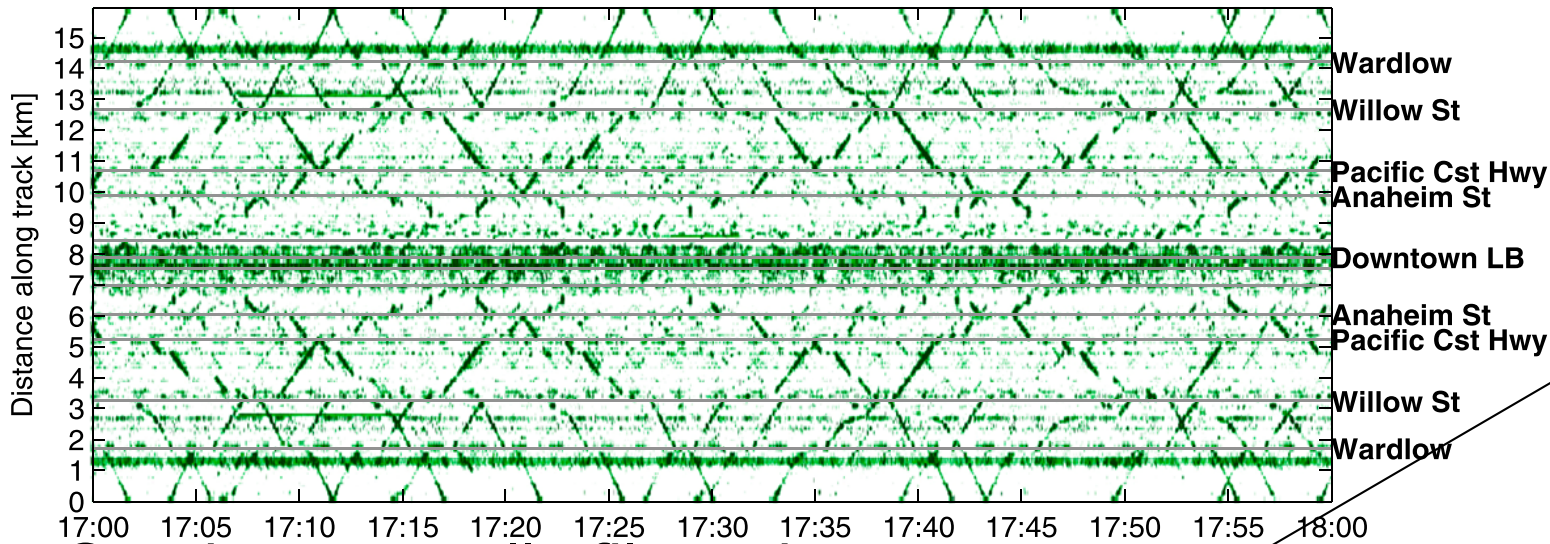


Long Beach Blue Line Metro

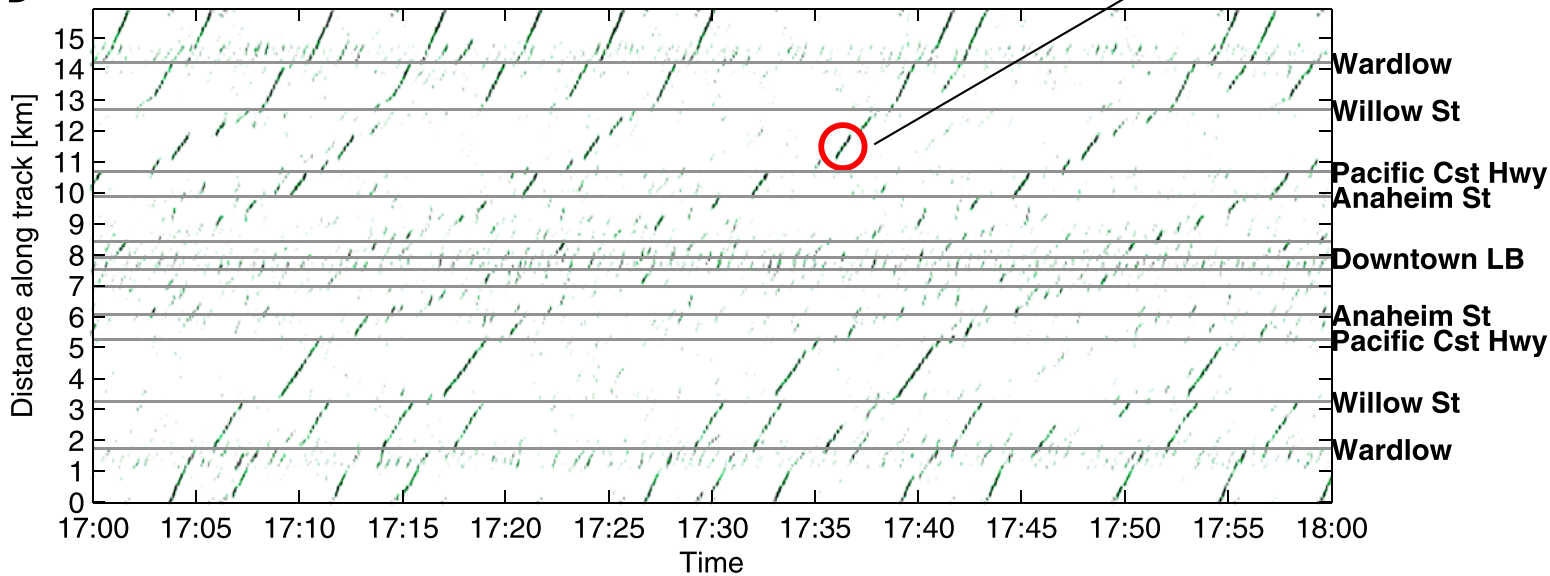


Seismic power along the metro track during rush hour

Raw seismic power



Spatiotemporally filtered power

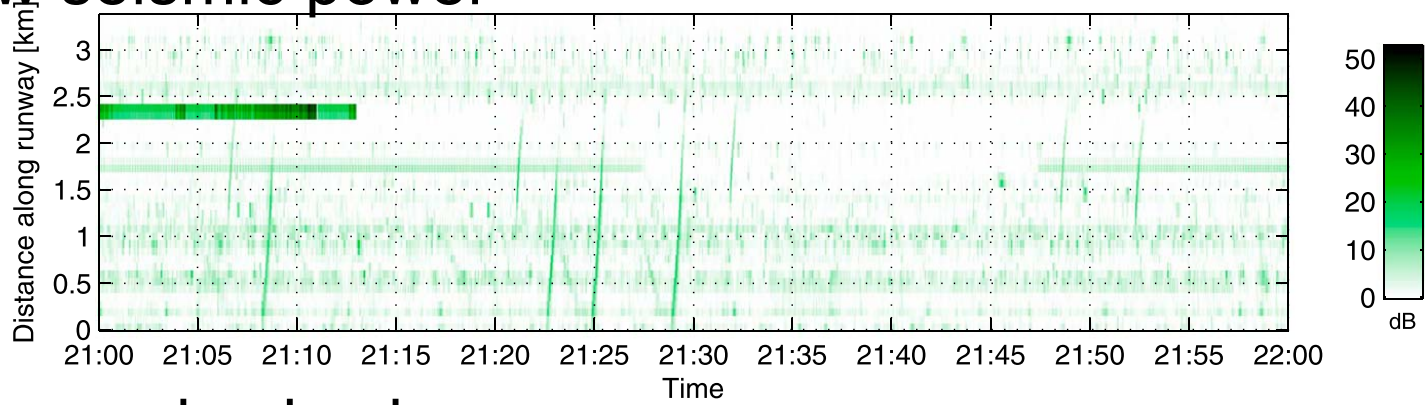




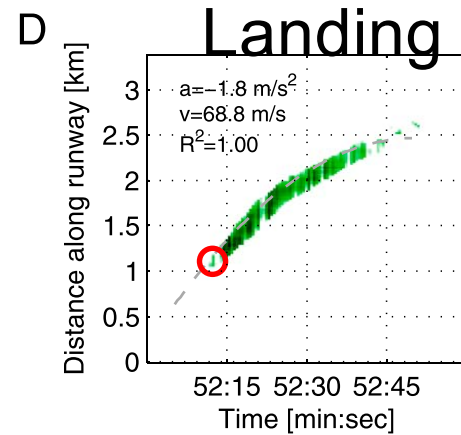
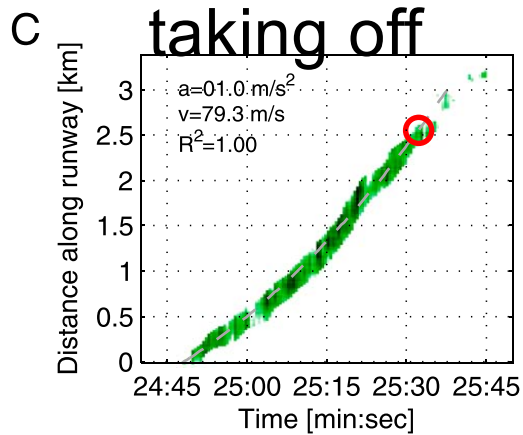
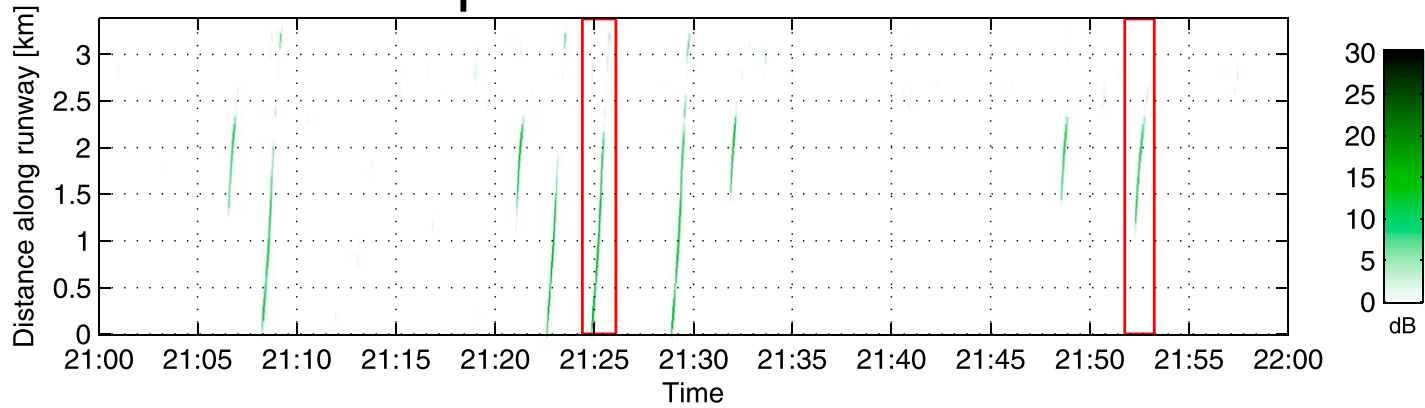
Watching airplanes with your feet (ears?)

Seismic power on runway

Raw seismic power



Processed seismic power.





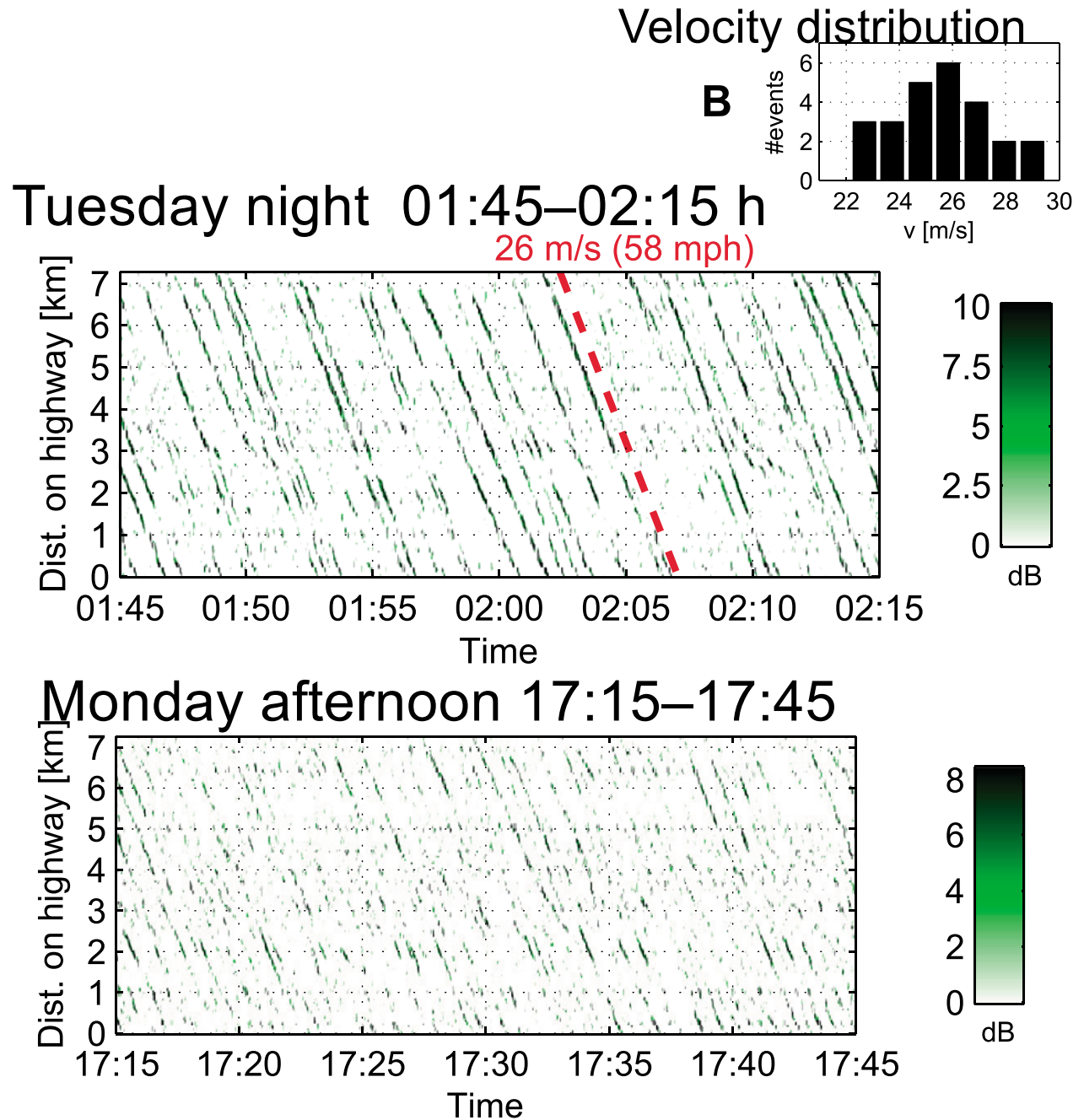
Observing the I-405

Seismic power for traffic monitoring

Processed seismic power along the I-405

Filtered for eastward moving sources

Currently other sensing techniques is favored.
Riahi, 2015

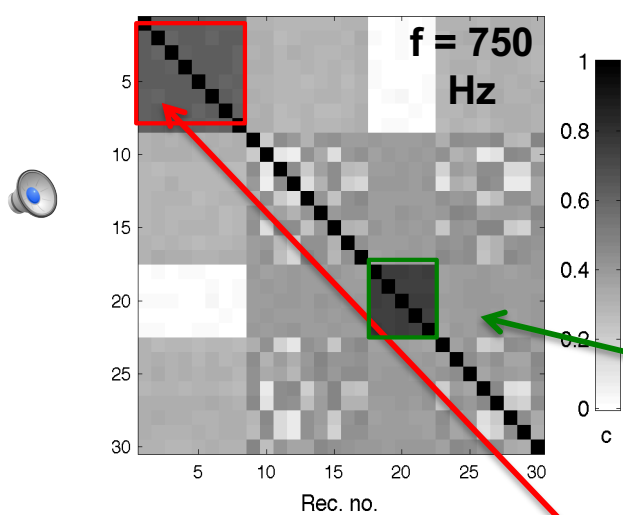


LOCATING WEAK SOURCES USING GRAPH SIGNAL PROCESSING

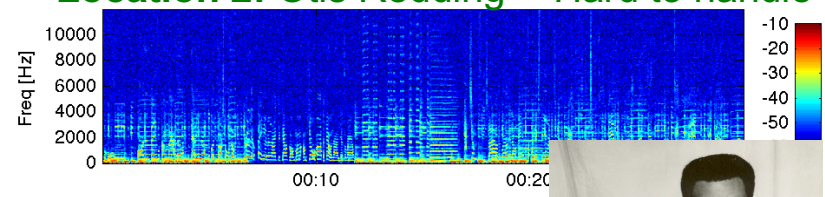
Riahi, Gerstoft (2017), Using Graph Clustering to Locate Sources within a Dense Sensor Array, Signal Processing 2017,

Graph Signal Processing for locating a source

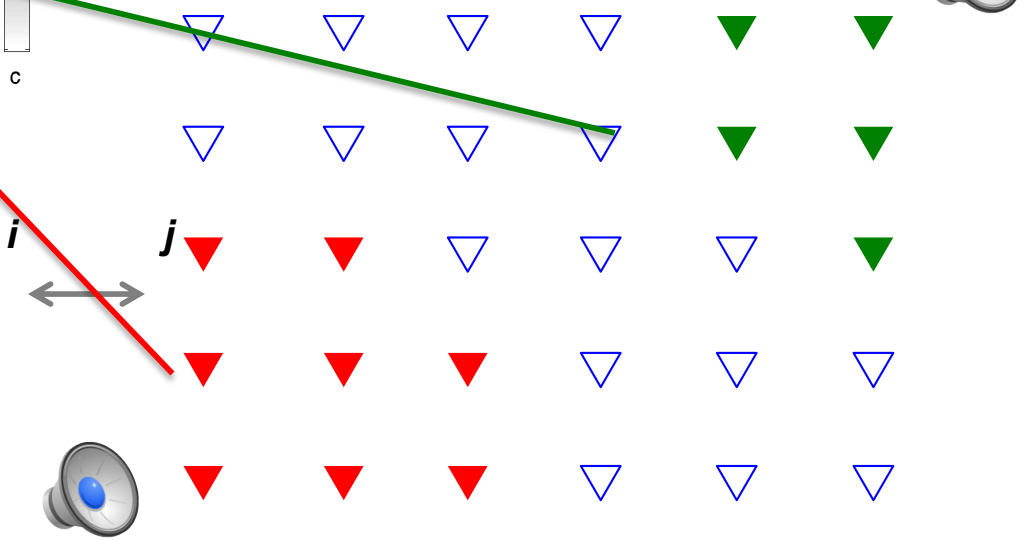
unsupervised



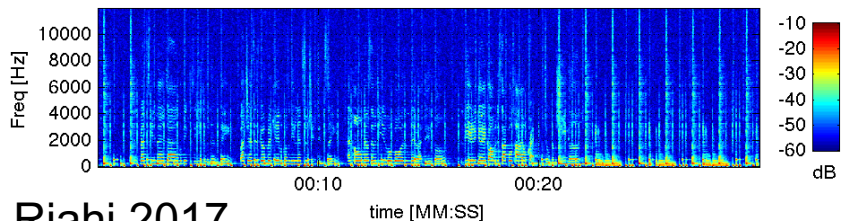
Location 2: Otis Redding - "Hard to handle"



30-microphone array



Location 1: Prince - "Sign o' the times"



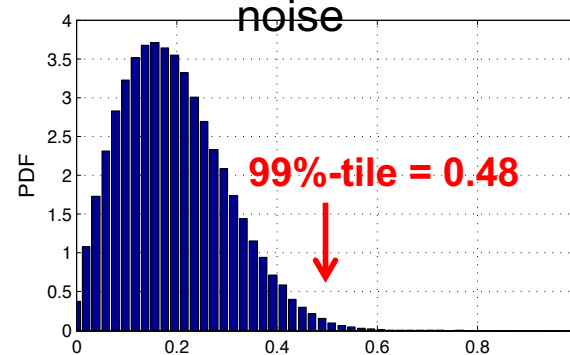
Spectral coherence

$$\hat{C}_{ij}(f) = \frac{1}{N} \sum_{t=1}^N X_i(f, t) \cdot \bar{X}_j(f, t)$$

(Normalization:

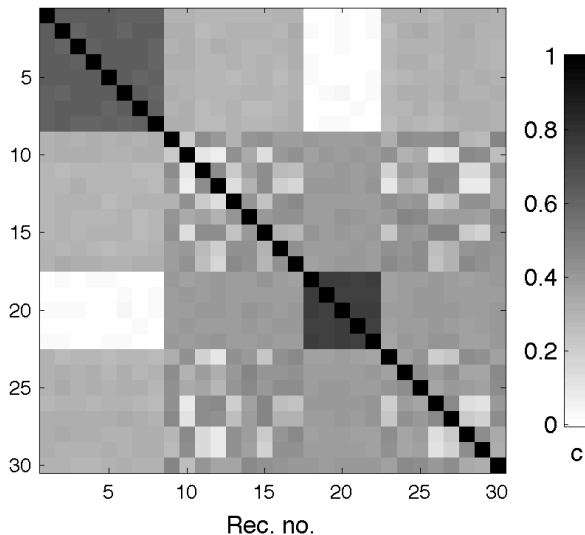
$$|X(f, t)|^2 = 1)$$

Distribution of $|C_{ij}|$ for incoherent noise

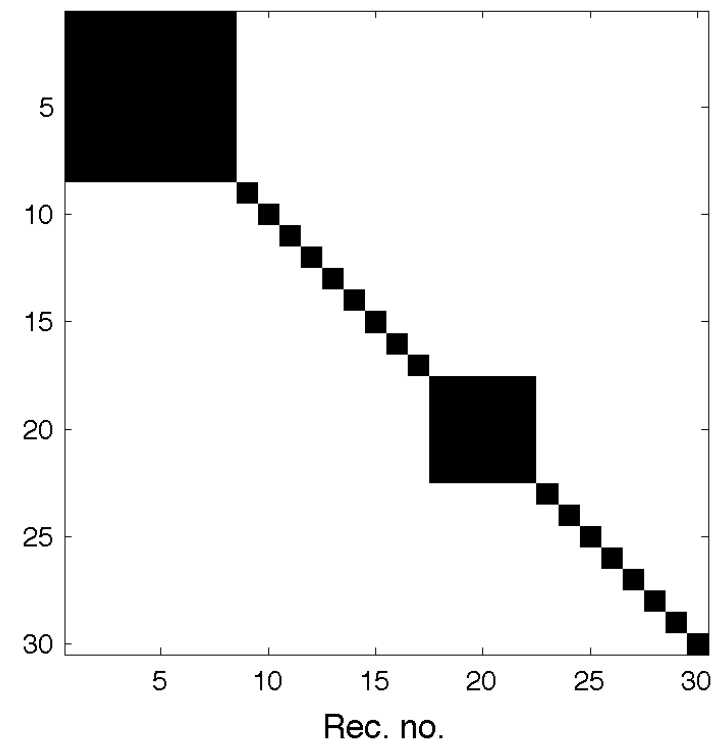


Each group is spatially coherent. But no temporal correlation between groups (i.e. different source)

Magnitude of spectral coherence for 30 sensors



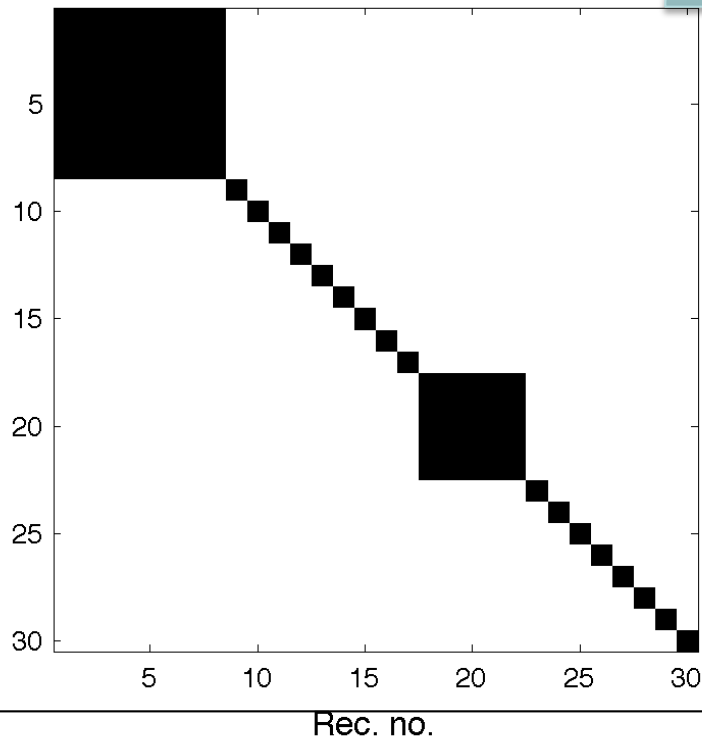
Statistically significant entries
=> **Connectivity matrix**



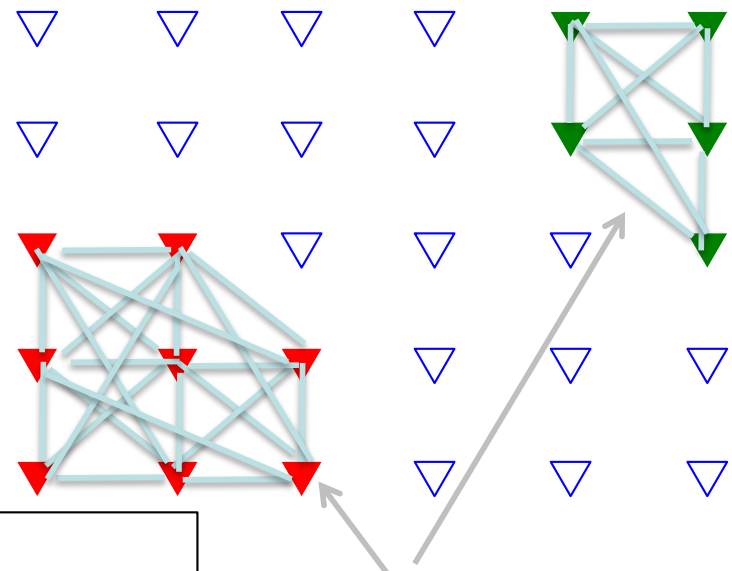
- Each sensor is a **node** in the graph. $|C_{ij}|$
- If **nodes** i and j are significantly correlated $|C_{ij}| > \xi$, then they share an **edge**.

Two sources in the network

Statistically significant entries
=> **Connectivity matrix**



Graph with 30 nodes

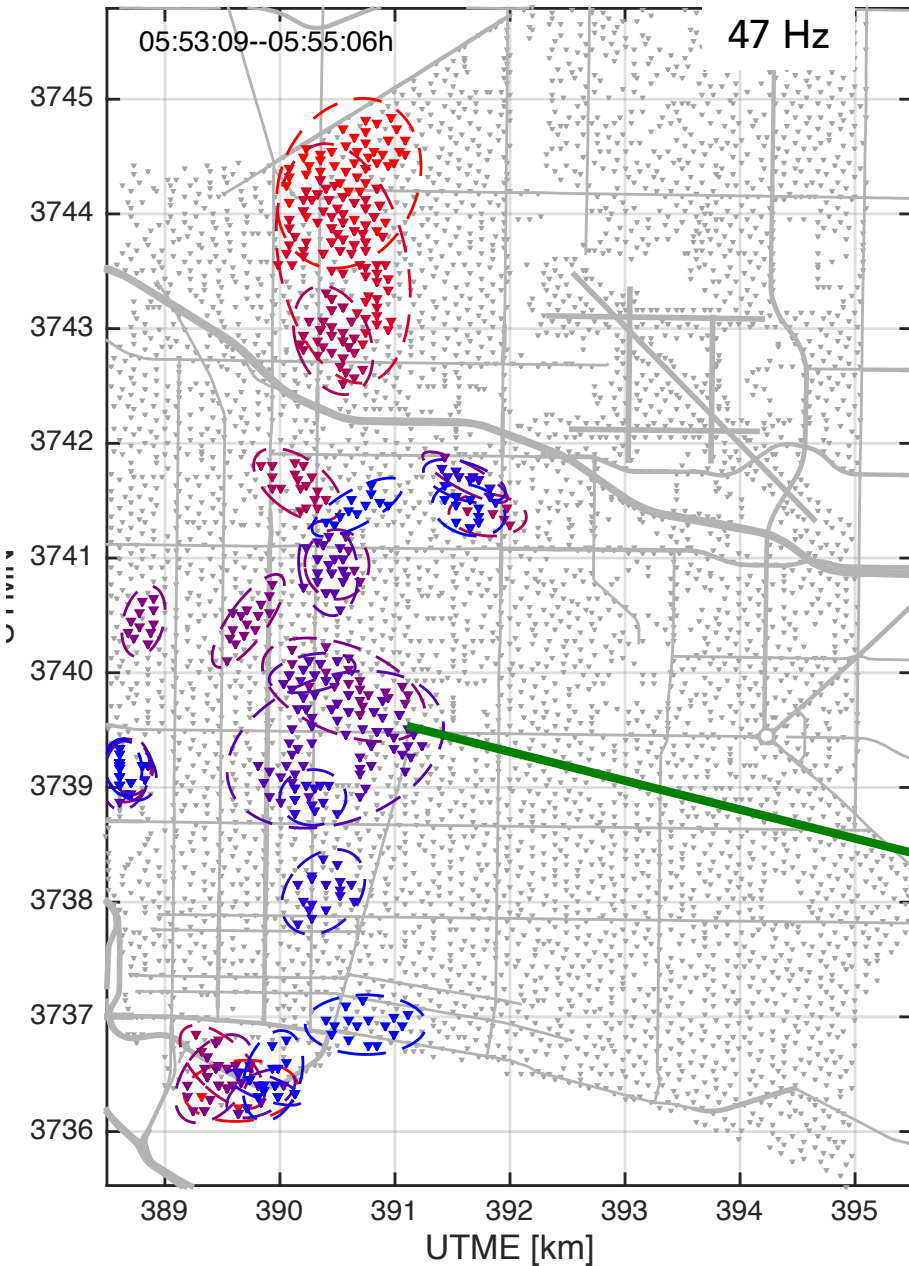


- Each sensor is a **node** in the graph.
- If **nodes** i and j are significantly correlated $|C_{ij}| > \xi$, then they share an **edge**.
- A **subgraph** has high spatial coherence across a subarray (=> likely a source nearby).

Connected subgraphs:

5 nodes and 9 edges

8 nodes and 20 edges



Helicopter rotor noise (seismo-acoustic coupling)

Several peaks consistent with helicopter rotor harmonics (20-100 Hz).

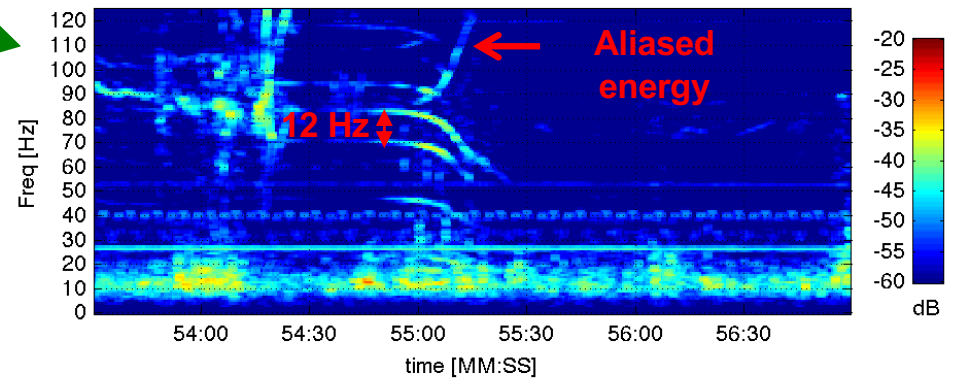
Doppler shift

$$f_{\text{high}}/f_{\text{low}} = (v_0 + v)/(v_0 - v) \approx 1.4 \text{ i.e. } v \approx 250 \text{ km/h}$$

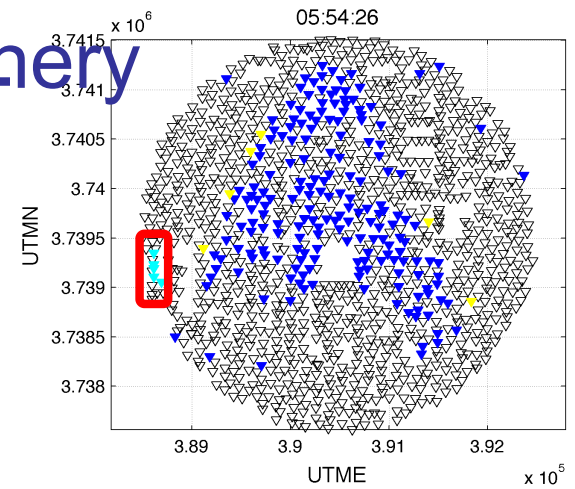
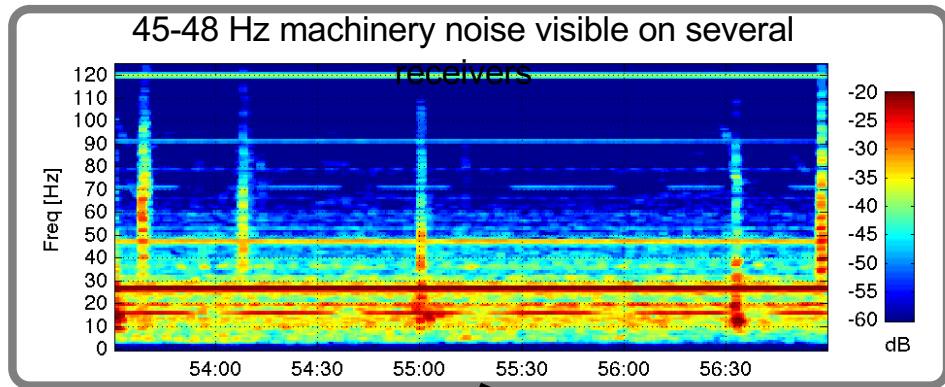
Speed over ground $7\text{km}/2\text{min} = 210\text{km/h}$



- ✓ Rotor frequencies
- ✓ Doppler frequency shift
- ✓ Movement in map



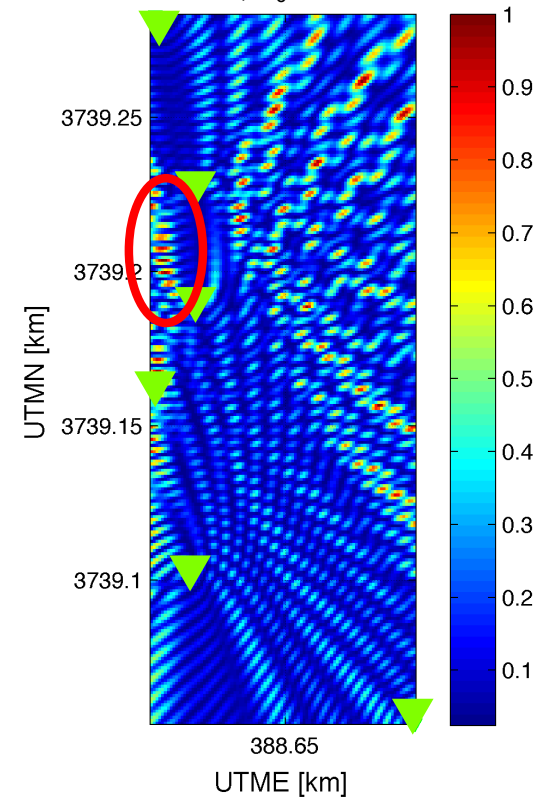
Example: Urban sounds rotating machinery



Location of mutually coherent receivers



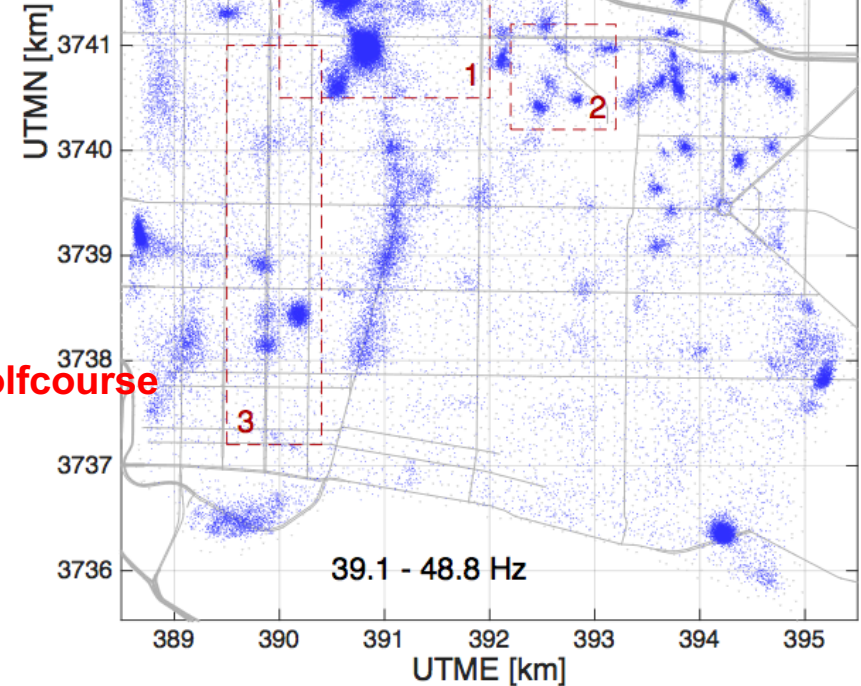
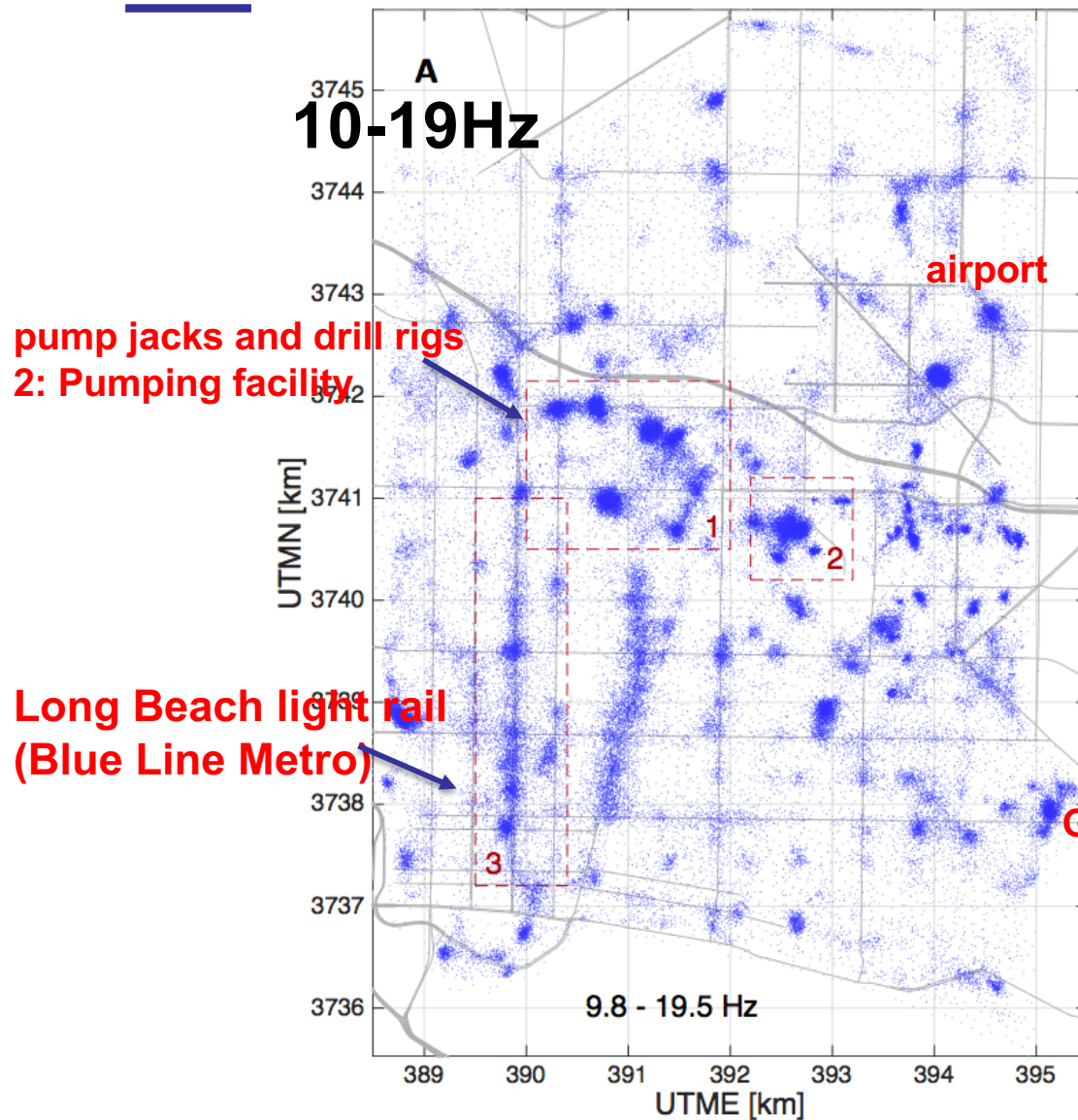
Matched-field processing
47Hz, $c_0=340$ m/s



Matched-field processing

- Wavelength = $340/47 = 7$ m
- Long Beach min. station spacing ≈ 70 m
- Seismic medium heterogeneities unknown.

Clusters on March 10



Based on 9400 time windows x 10 frequency bins.

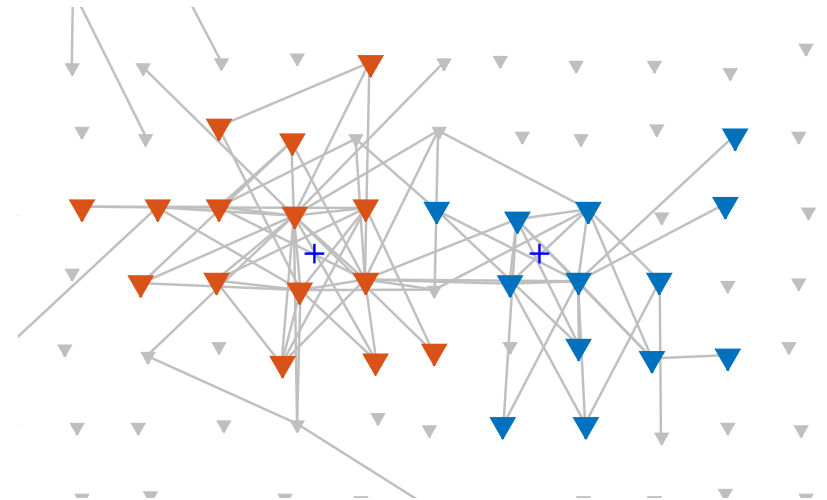
Each dot is the center of a cluster. 90% of the clusters cover <1.5% of the area.

Few false detections

450'000 sensor clusters detected in total

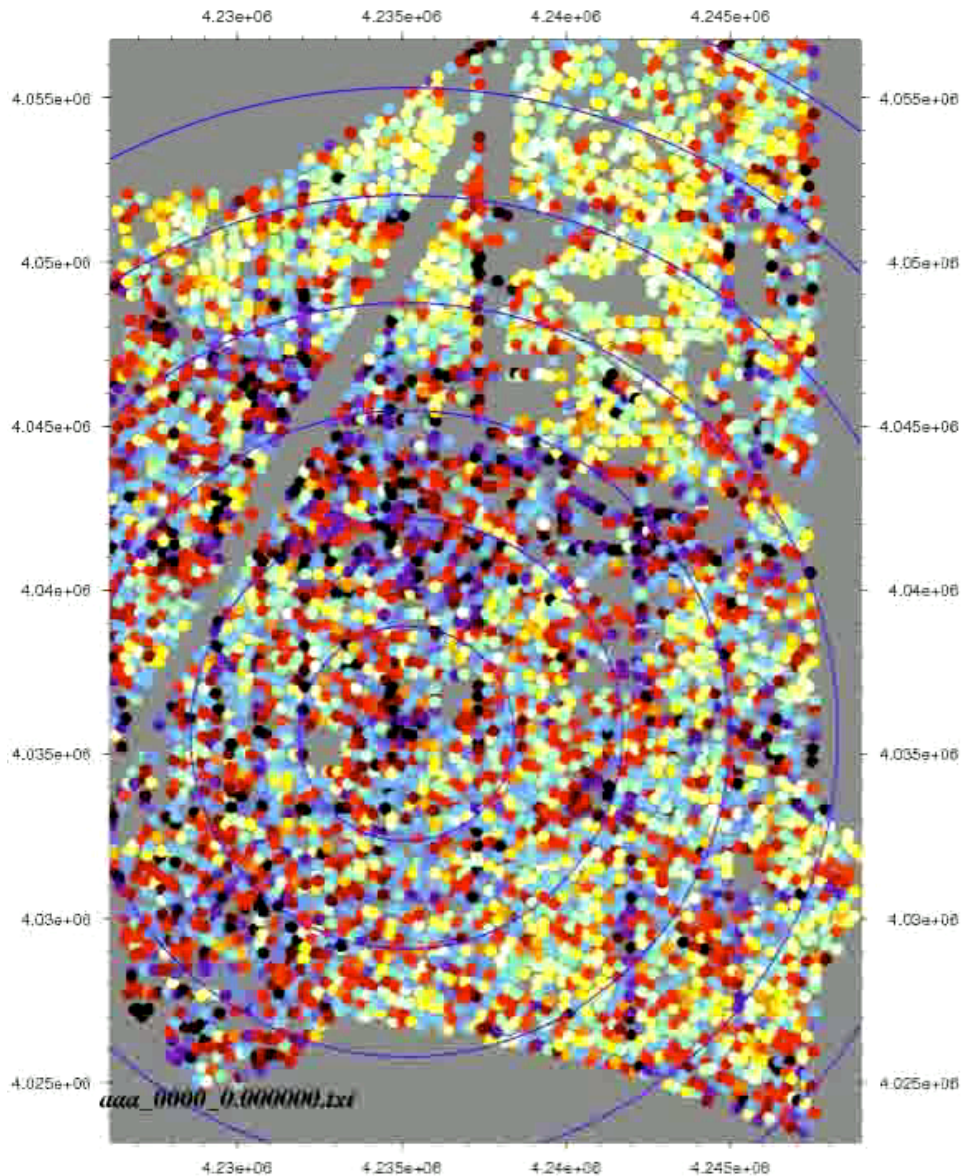
Conclusions

- ✓ Pair-wise coherence defines a network across array sensors.
- ✓ Weak within-array sources induce topology on that network. This topology is used to approximately localize weak sources.
- ✓ Model-free approach
- ✓ Tested on large-scale empirical geophone data

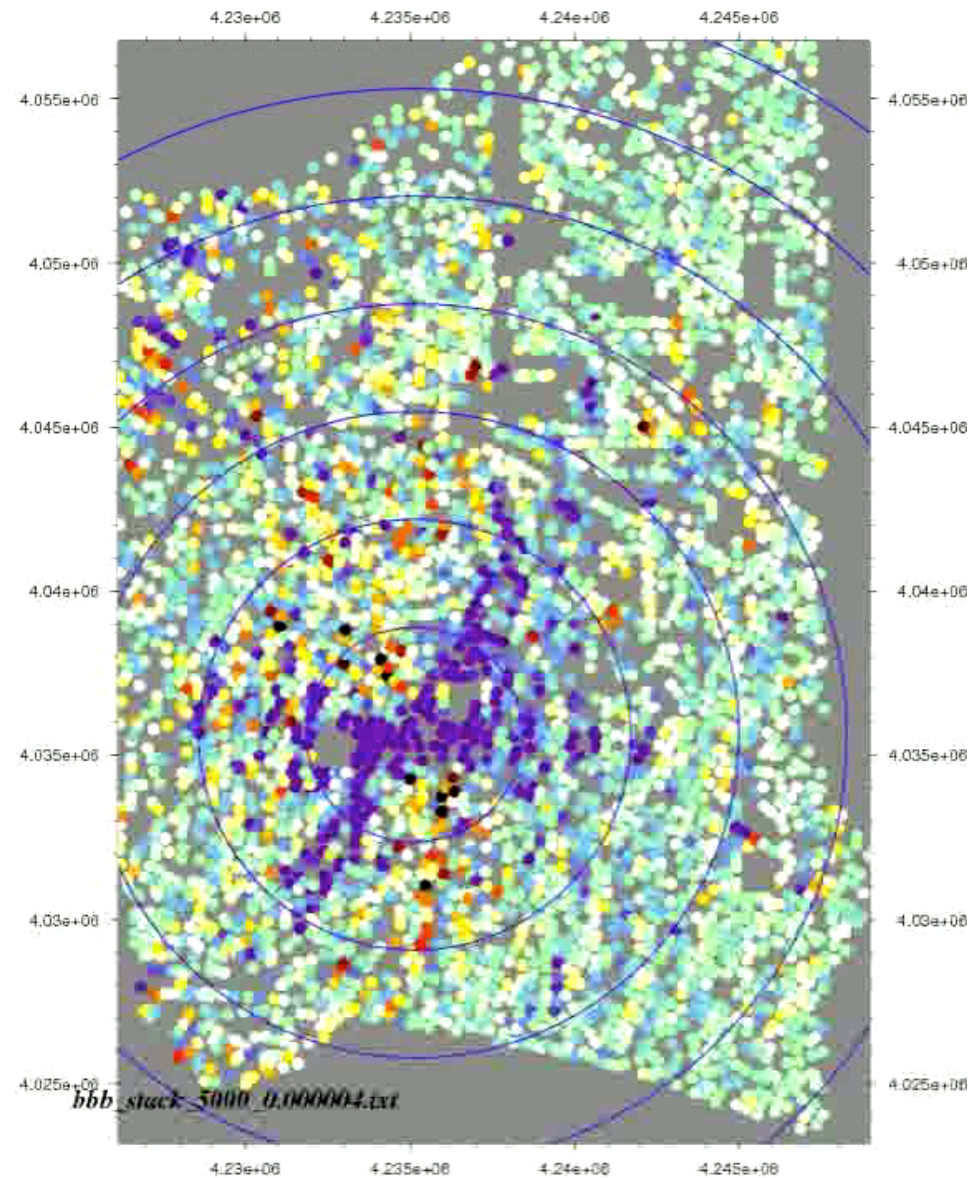


Constructing Greens Functions from noise

Vibro-source



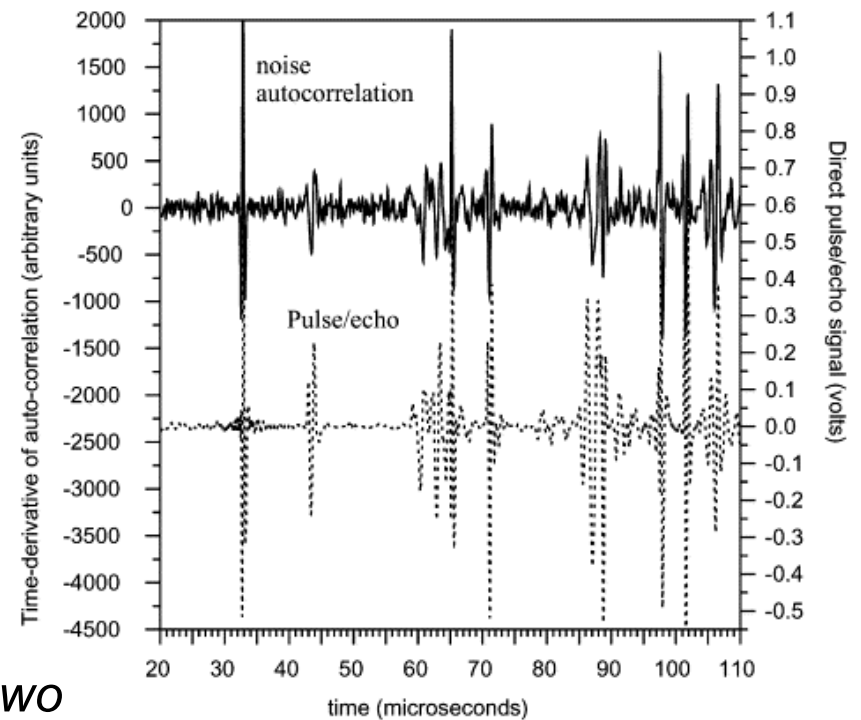
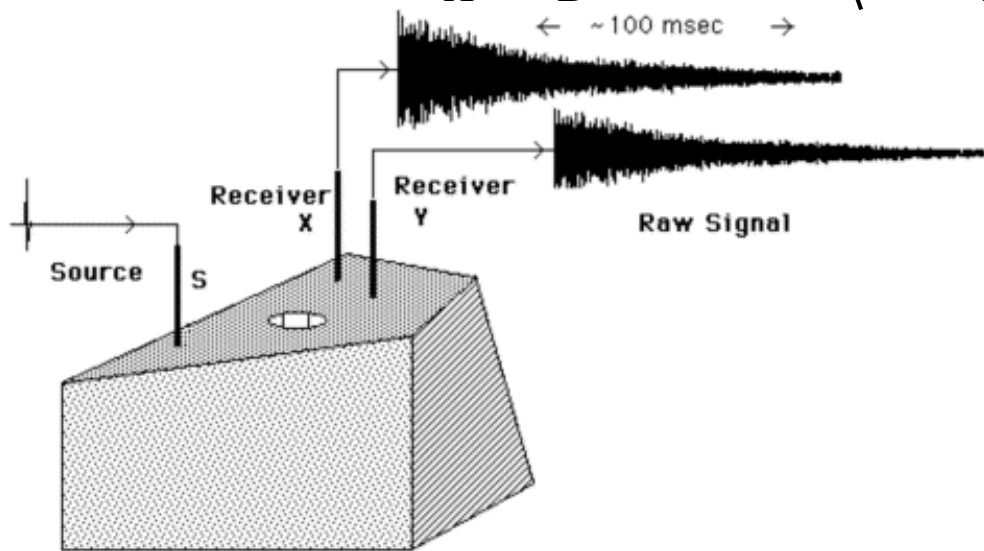
From ambient noise



Coherent signals from noise data

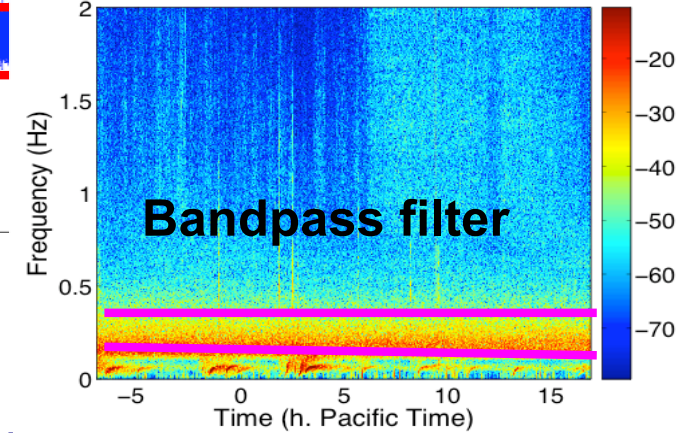
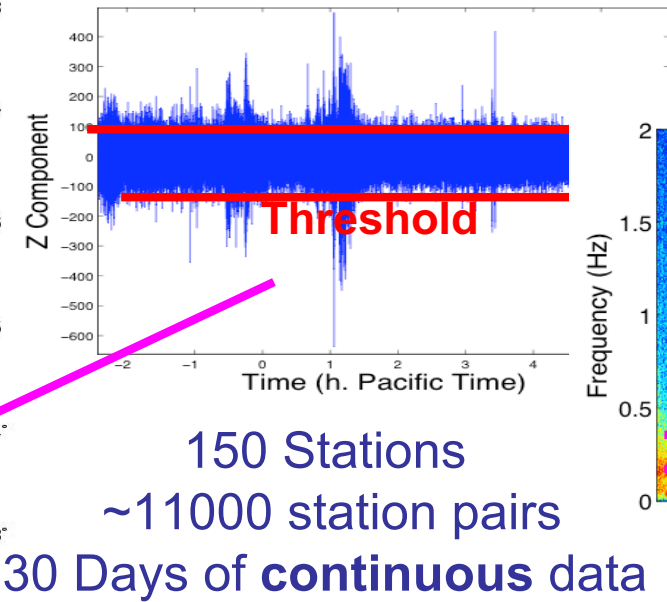
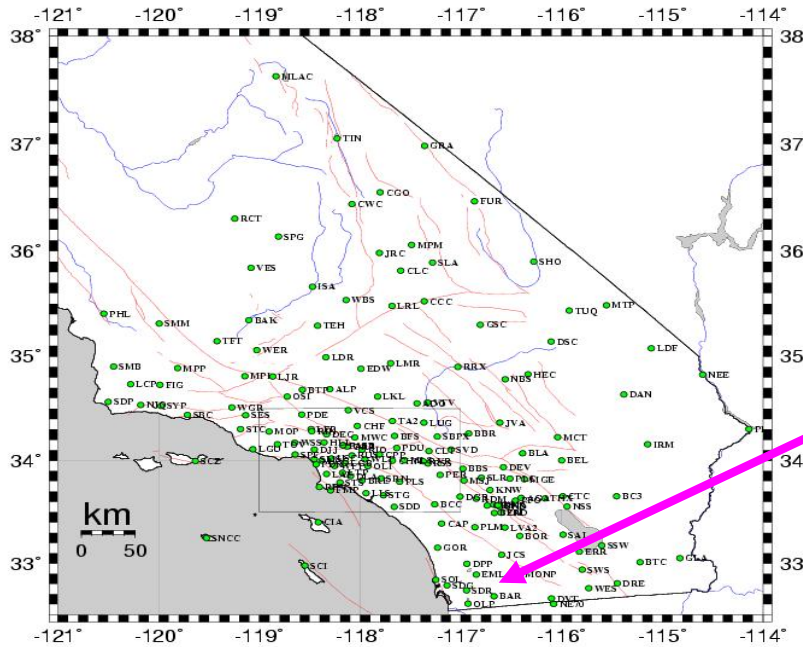
The Green's function emerges from the cross-correlation of the diffuse wave field at two points of observation:

$$G(\mathbf{x}_A, \mathbf{x}_B, t) \propto \langle v(\mathbf{x}_A, -t) * v(\mathbf{x}_B, t) \rangle$$

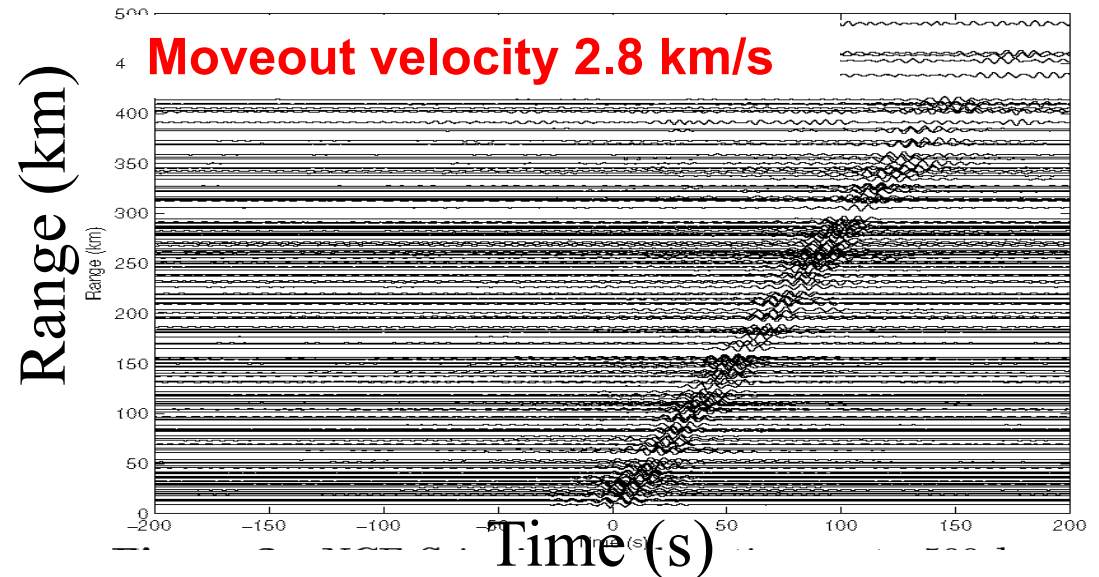


“By cross-correlating ambient noise recorded at two locations, the Green’s function between these two locations can be reconstructed”. (Claerbout 1999, Weaver 2001.)

Seismic interferometry and in southern California

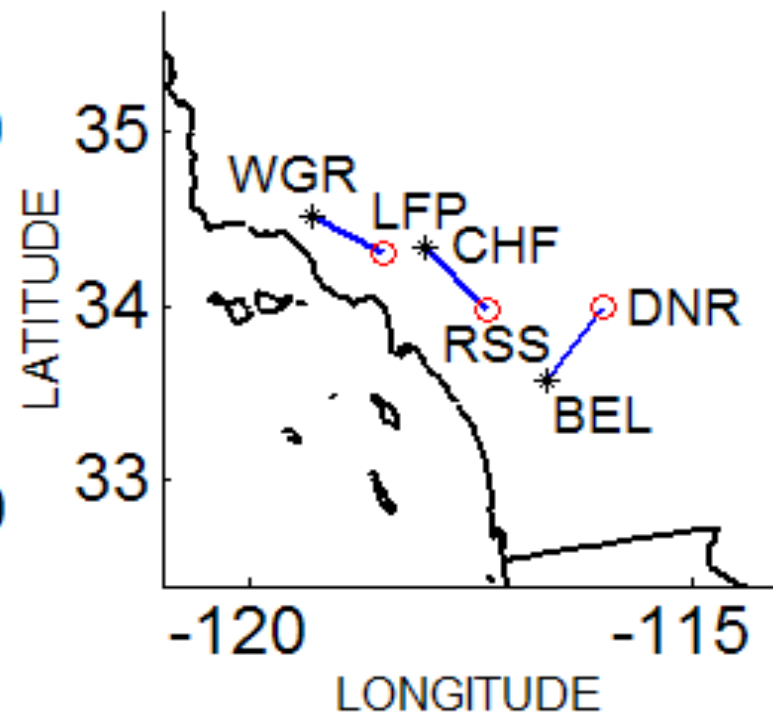
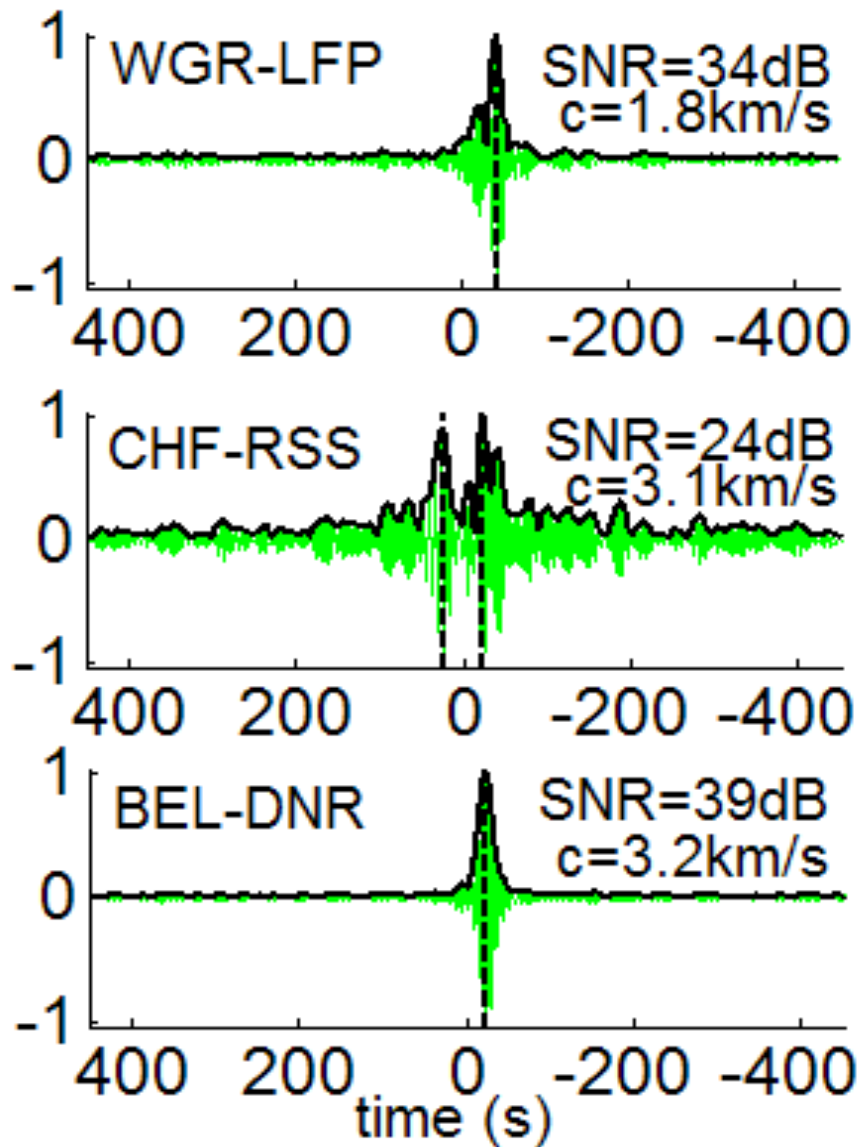


Result of noise cross correlation order with range



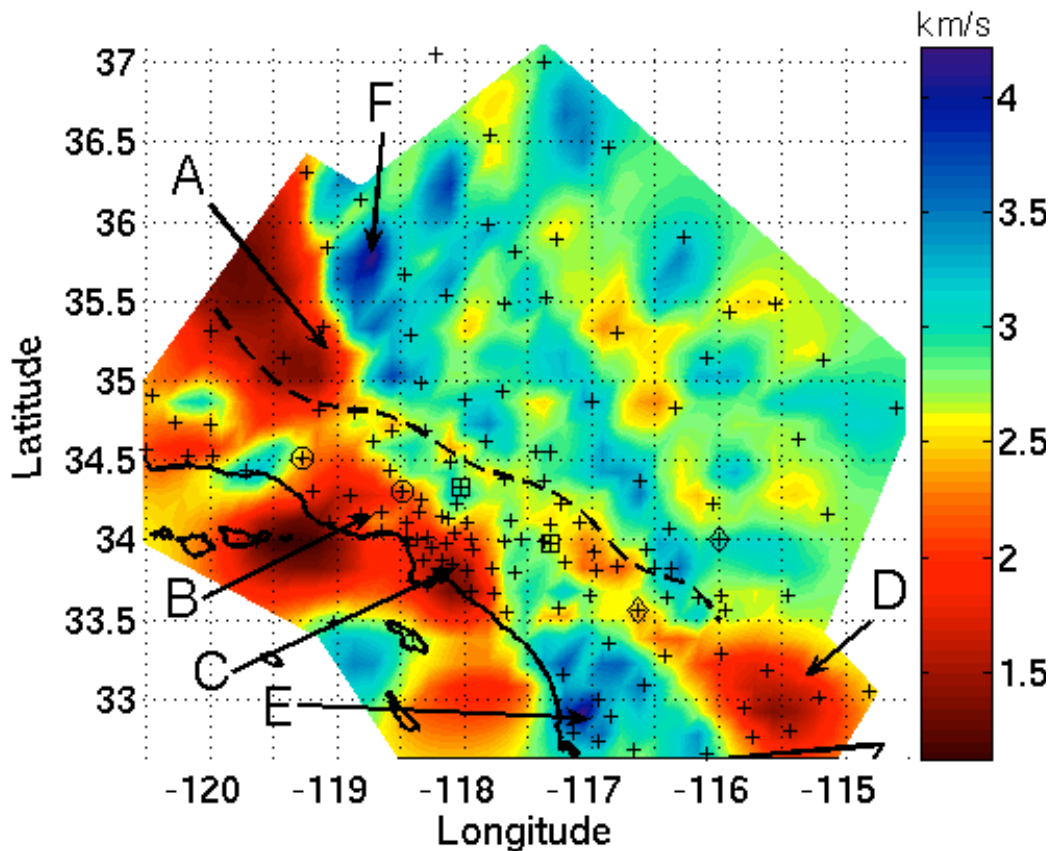
Individual paths have different travel time=> tomography
Sabra, GRL 2005; Gerstoft, Geophysics 2006

2D variations of the noise Rayleigh wave



Ambient noise Surface wave Tomography

Tomographic map

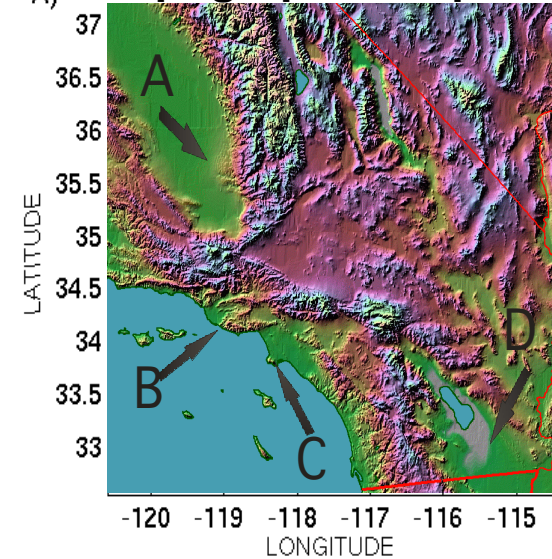


Low Velocity Region~Sedimentary basins A: San Joaquin, B: Ventura, C: L.A., D: Salton Sea

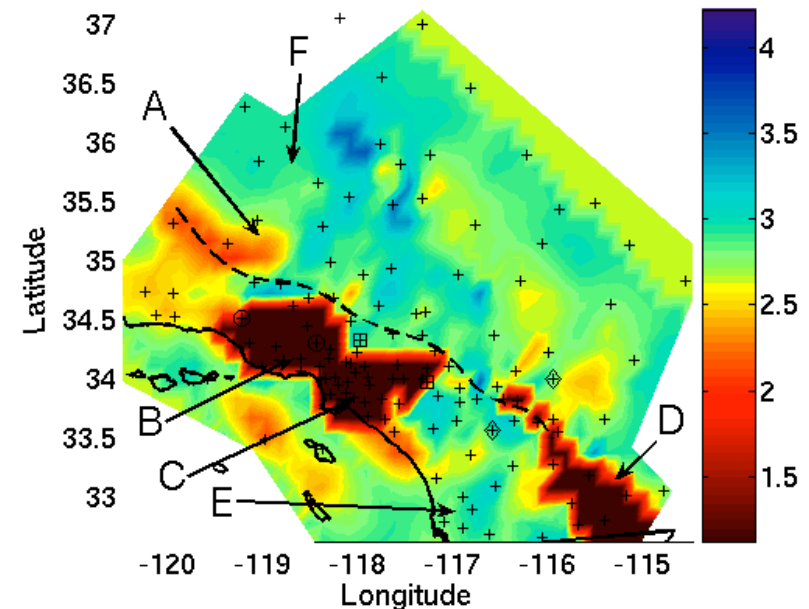
One month of ambient noise can replace 10 years of earthquake tomography!

Sabra, GRL 2005,
Gerstoff et al 2006

A) Topographic map



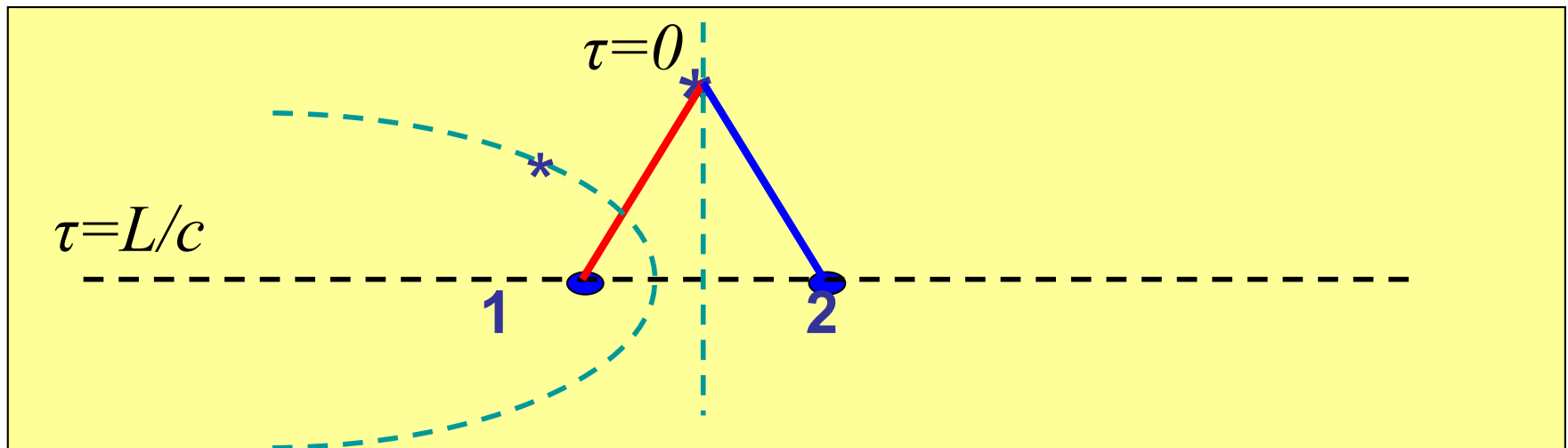
3D Earth model



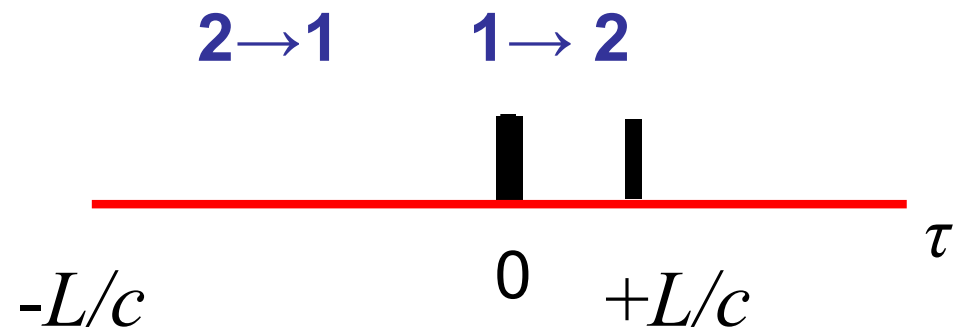
Free space noise correlation (3D)

$$C_{12}(\tau) = \int_{-\infty}^{\infty} P(\mathbf{r}_1, t) P(\mathbf{r}_2, t + \tau) dt.$$

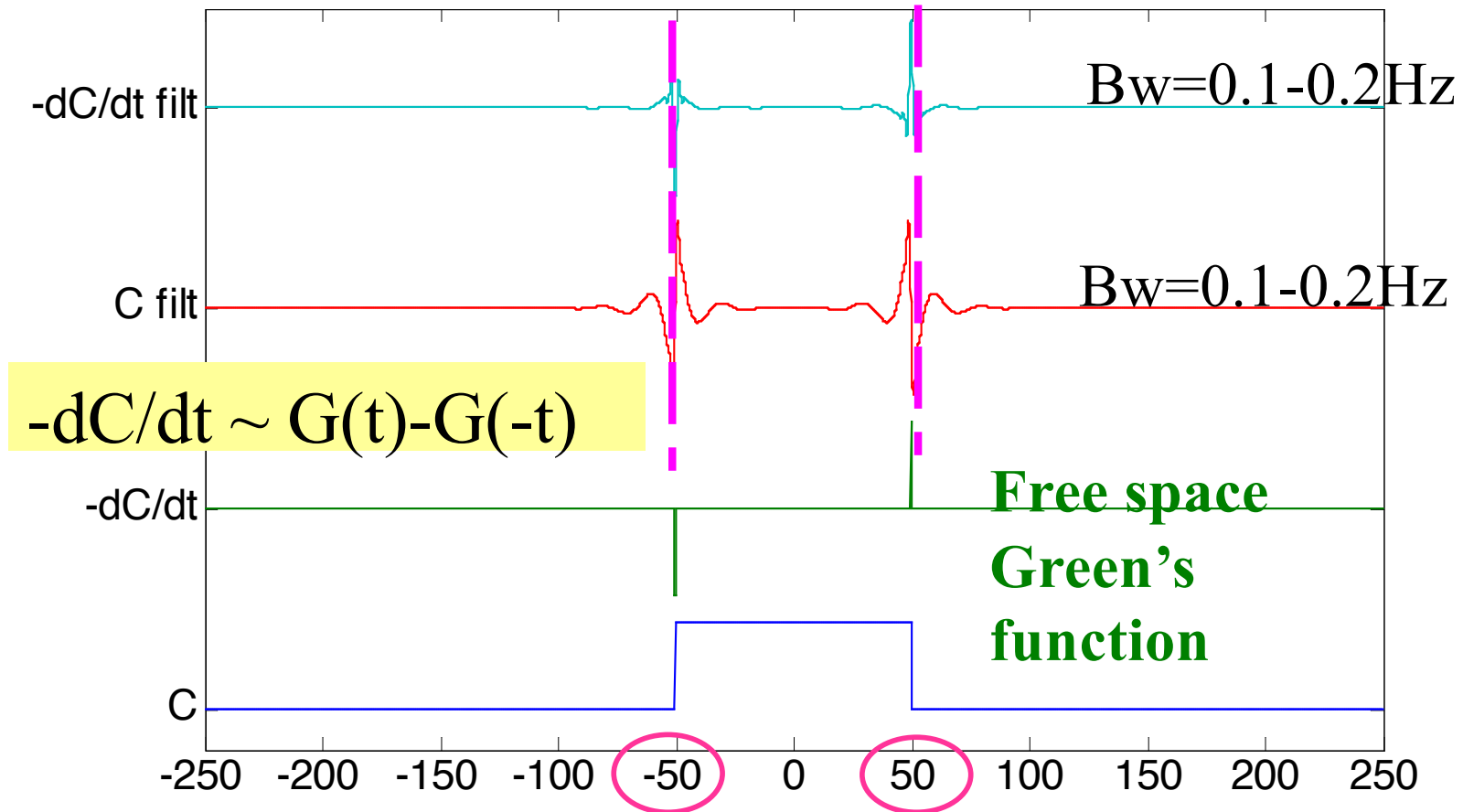
$$\frac{dC_{12}(\tau)}{d\tau} \propto -G(t) + G(-t)$$



Sources yielding constant time-delay τ lay on same hyperbola



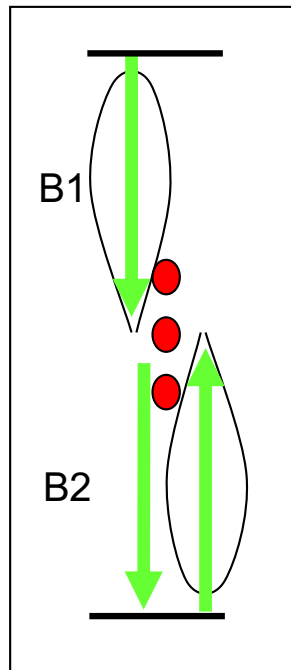
C, dC/dt, band-limited signal



With cross-correlation process the phase of the source signal is removed,
→ Arrival time is given by the center of the pulse (envelope maximum)
Isotropic noise distribution → Symmetric Correlation function.

Passive fathometer

Using ambient noise on a drifting array we can map the bottom properties



Siderius et al., JASA 2006,
Gerstoft et al., JASA 2008,
Harrison, JASA 2009,
Traer et al., JASA 2009, 2010, 2011
Siderius et al., JASA 2010

Endfire beamforming

Wind and waves make sound coming from all directions

Beamforming with a vertical array allows the sound coming from directions other than endfire to be greatly reduced.

This makes short time-averaging possible- an important component for practical application.

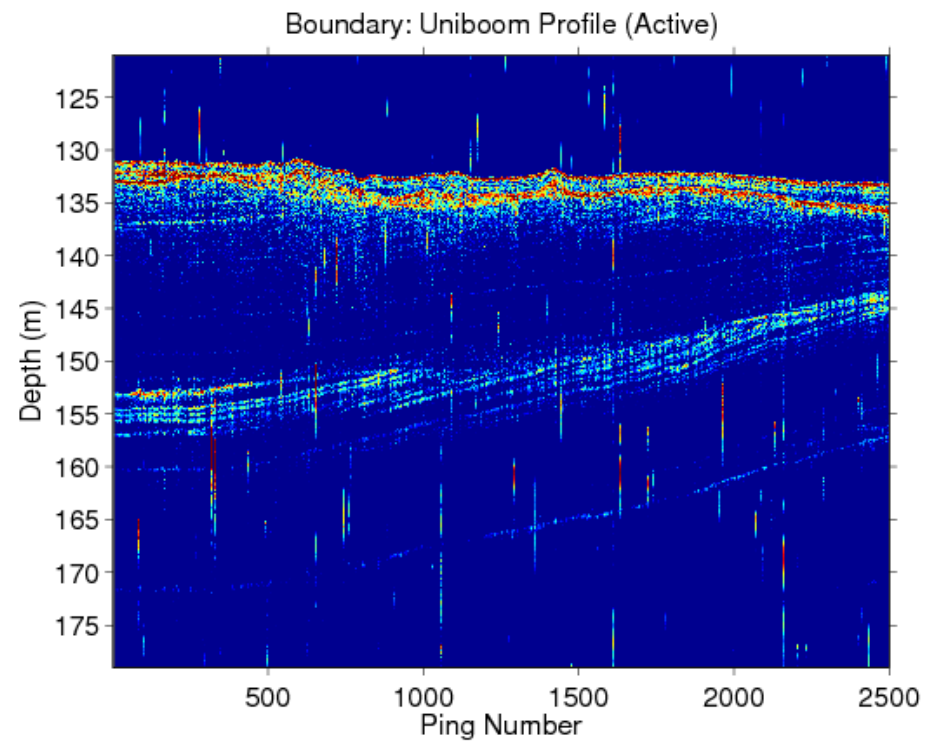
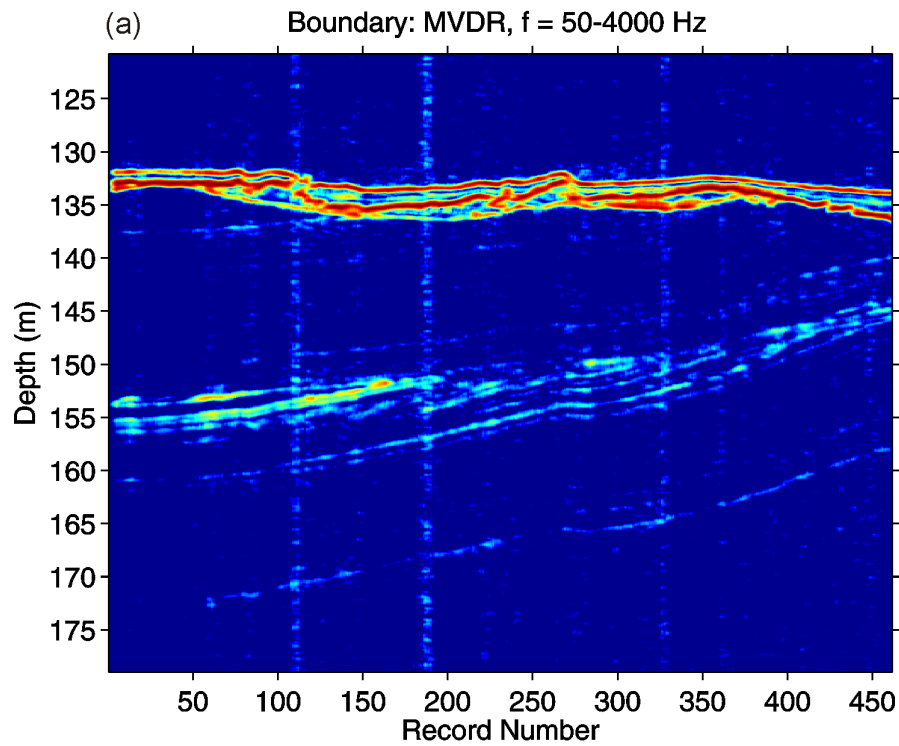
← Vertical array

The diagram illustrates the concept of endfire beamforming. At the top, a row of yellow sun-like icons represents sound sources on the water surface, with white curved lines indicating sound waves spreading out. Below this, a vertical array of hydrophones is shown as a dashed line. A cone of light-colored sound waves is directed downwards from the array, representing the beamformed signal. The background is a gradient from light blue at the top to dark blue at the bottom, with a brown seabed at the very bottom.

Passive fathometer

Ambient noise 50-4000 Hz

Boomer



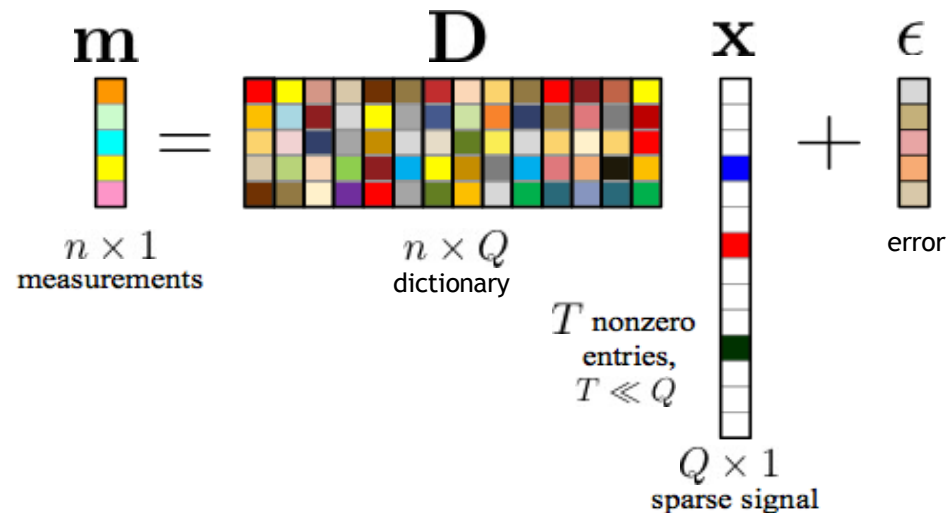
Adaptive processing gives better resolution of reflections

Sparse models and dictionaries

- Sparse modeling assumes each signal model can be reconstructed from a few vectors from a large set of vectors, called a dictionary \mathbf{D}
- Adds auxiliary sparse model to measurement model

$$\mathbf{d} = \mathbf{A}\mathbf{m} + \mathbf{n}, \quad \mathbf{m} \approx \mathbf{D}\mathbf{x} \quad \text{and} \quad |\mathbf{x}| \ll Q$$

- Optimization changes from estimating \mathbf{m} to estimating sparse coefficients \mathbf{x}



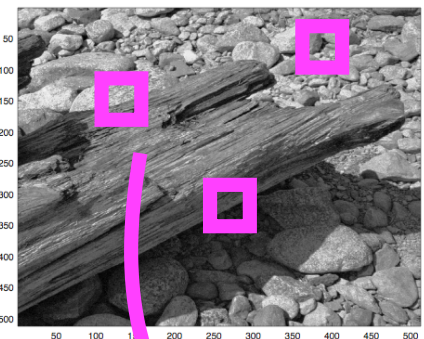
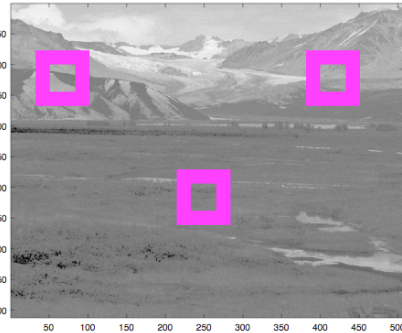
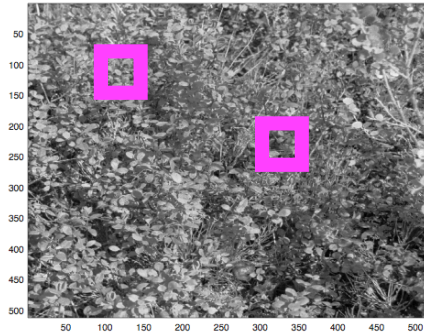
- Sparse objective: $\min_{\mathbf{x}} \|\mathbf{A}\mathbf{D}\mathbf{x} - \mathbf{d}\|_2$ subject to $\|\mathbf{x}\|_0 \leq T$

Dictionary learning and sparsity

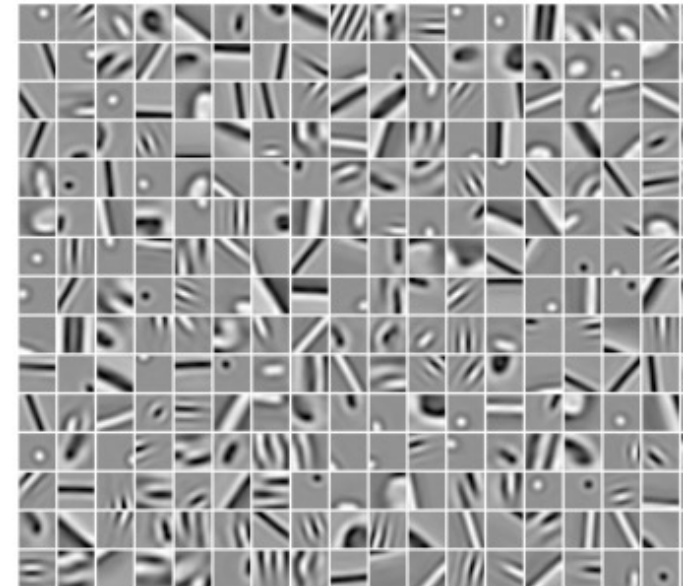
unsupervised

- Dictionary learning obtains "optimal" sparse modeling dictionaries directly from data
- Dictionary learning was developed in neuroscience (a.k.a. sparse coding) to help understand mammalian visual cortex structure
- Assumes (1) Redundancy in data: image patches are repetitions of a few elemental shapes; and (2) Sparsity: each patch is represented with few atoms from dictionary

"Natural" images, patches shown in magenta



Learn dictionary \mathbf{D} describing $\mathbf{Y} = [\mathbf{y}_1, \dots, \mathbf{y}_I]$



Olshausen 2009

- Each patch is signal \mathbf{y}_i
- Set of all patches $\mathbf{Y} = [\mathbf{y}_1, \dots, \mathbf{y}_I]$

Sparse model for patch \mathbf{y}_i composed of few atoms from \mathbf{D}

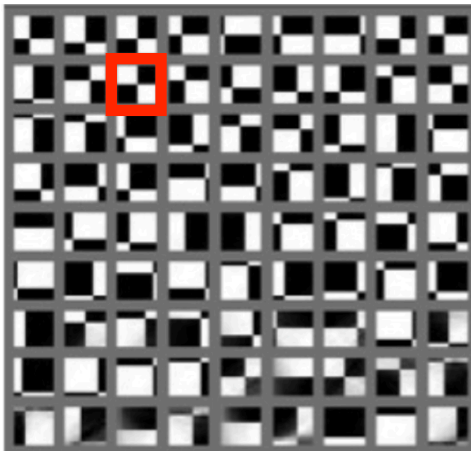
$$\hat{\mathbf{x}}_i = \arg \min_{\mathbf{x}_i} \|\mathbf{y}_i - \mathbf{D}\mathbf{x}_i\|_2 \quad \text{subject to} \quad \|\mathbf{x}_i\|_0 \leq T$$

$$\mathbf{y} = \begin{matrix} \text{patch} \\ \mathbf{x}_i \end{matrix} = \begin{matrix} \text{atom} \\ \mathbf{x}_1 \end{matrix} x_1 + \begin{matrix} \text{atom} \\ \mathbf{x}_2 \end{matrix} x_2 + \dots$$

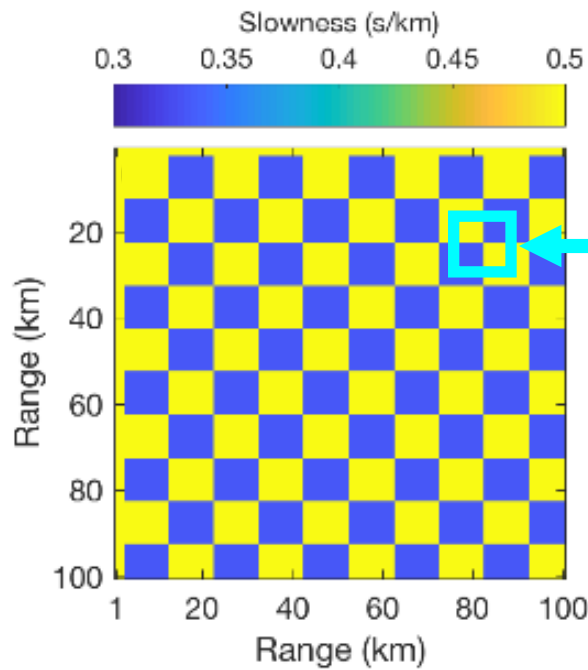
Bianco 2018, 2019

Checkerboard dictionary example

Dictionary \mathbf{D}



Slowness



$$\mathbf{y} = \mathbf{R}_i \mathbf{s} = \mathbf{D} \mathbf{x}_i$$

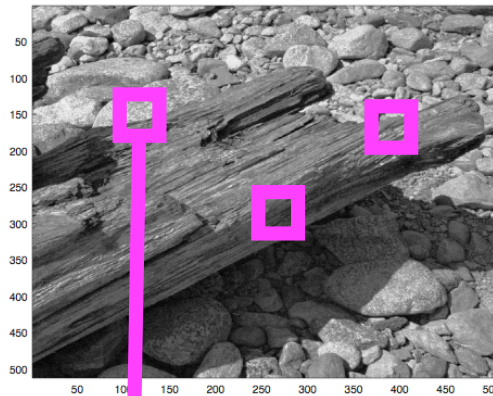
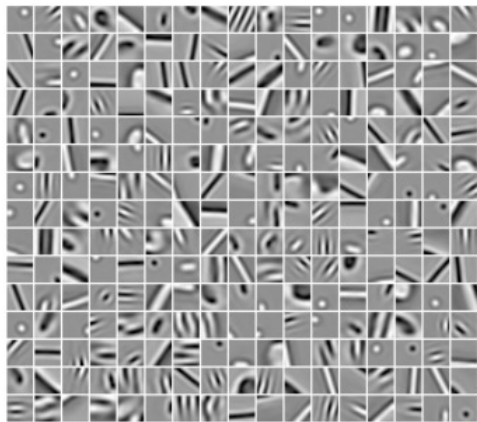
$$\mathbf{R}_i \mathbf{s} = \begin{bmatrix} \blacksquare & \square \\ \square & \blacksquare \\ \blacksquare & \square \\ \square & \blacksquare \end{bmatrix} \mathbf{s} = \mathbf{x}_i$$

10x10 pixel patches

$$\mathbf{D} \in \mathbb{R}^{n \times Q}$$

$$\mathbf{R}_i \in \{0, 1\}^{n \times N}$$

Natural image

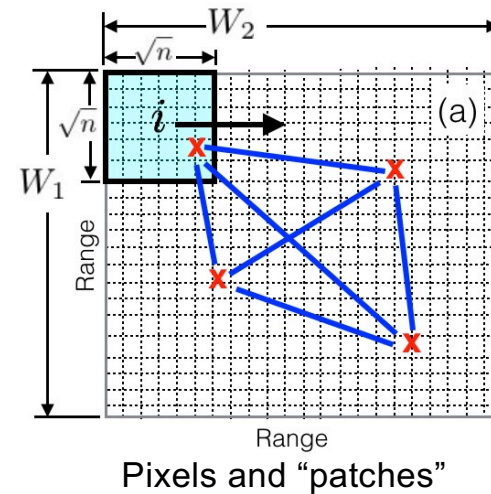
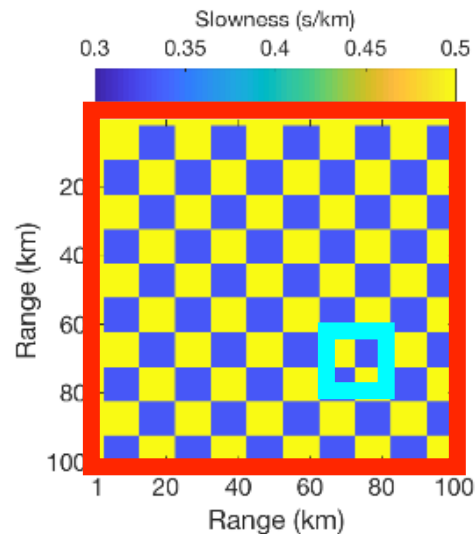


$$\hat{\mathbf{x}}_i = \arg \min_{\mathbf{x}_i} \|\mathbf{y}_i - \mathbf{D} \mathbf{x}_i\|_2 \quad \text{subject to} \quad \|\mathbf{x}_i\|_0 \leq T$$

$$\mathbf{y} = \begin{bmatrix} \text{log patch} \end{bmatrix} = \begin{bmatrix} \text{horizontal patch} \end{bmatrix} x_1 + \begin{bmatrix} \text{diagonal patch} \end{bmatrix} x_2 + \dots$$

Bianco 2018, 2019

LST slowness image and sampling



Slowness map and measurements

- stations in red
- rays in blue

Slowness map and sampling:

- Discrete slowness map $N=W_1 \times W_2$ pixels
- I overlapping $\sqrt{n} \times \sqrt{n}$ pixel patches
- M straight-ray paths

Tomography matrix
(straight ray)

$$\mathbf{A} \in \mathbb{R}^{M \times N}$$

Slowness dictionary

$$\mathbf{D} \in \mathbb{R}^{n \times Q}$$

$$Q \ll I$$

“Local” model

$$\hat{\mathbf{x}}_i = \arg \min_{\mathbf{x}_i} \|\mathbf{R}_i \mathbf{s}_s - \mathbf{D} \mathbf{x}_i\|_2^2 \text{ subject to } \|\mathbf{x}_i\|_0 = T$$

“Global” model

$$\mathbf{t} = \mathbf{A} \mathbf{s}_g + \epsilon, \quad \hat{\mathbf{s}}_g = \arg \min_{\mathbf{s}_g} \|\mathbf{t} - \mathbf{A} \mathbf{s}_g\|_2^2 + \lambda_1 \|\mathbf{s}_g - \mathbf{s}_s\|_2^2,$$

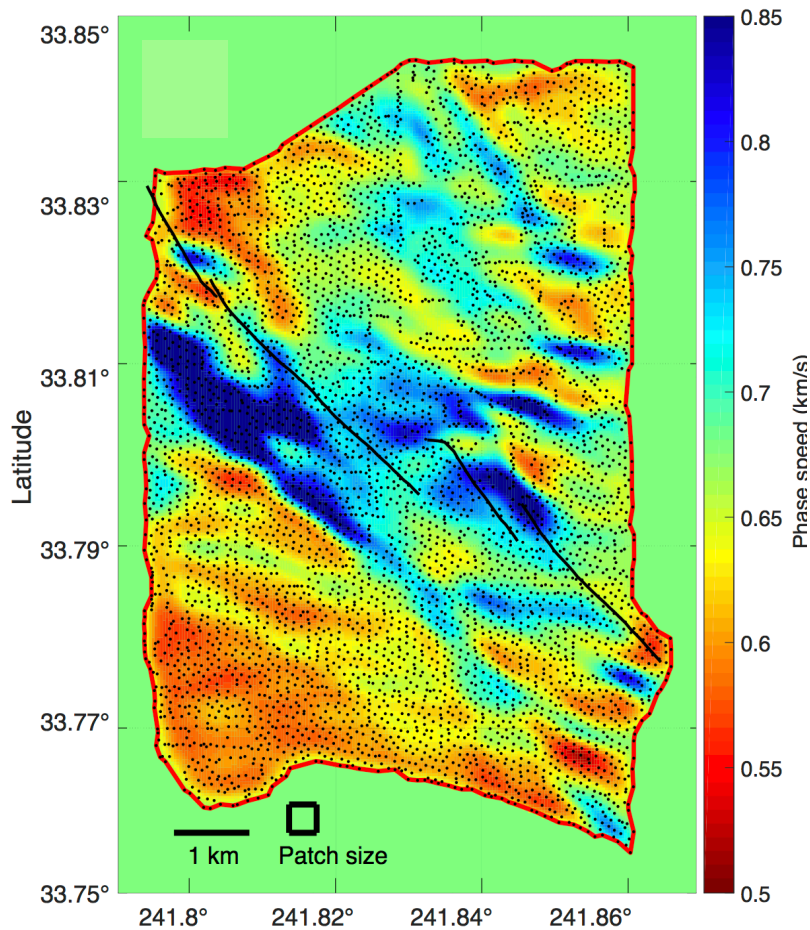
Bayesian formulation

LST versus conventional tomography

Both use same travel times (from Fan-Chi Lin),

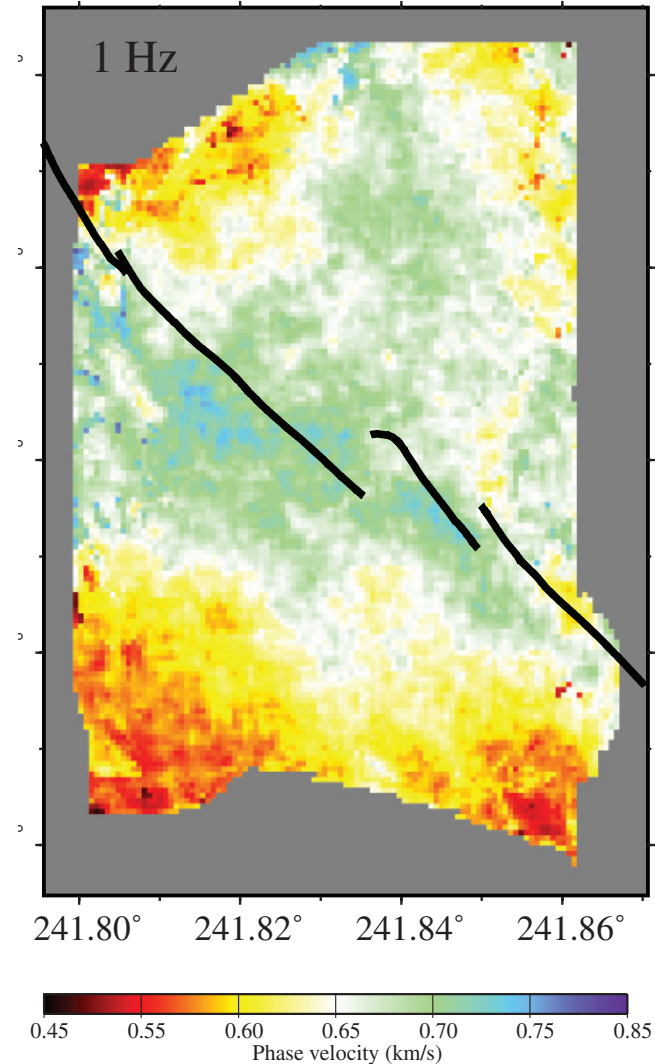
unsupervised

LST 3 mill rays



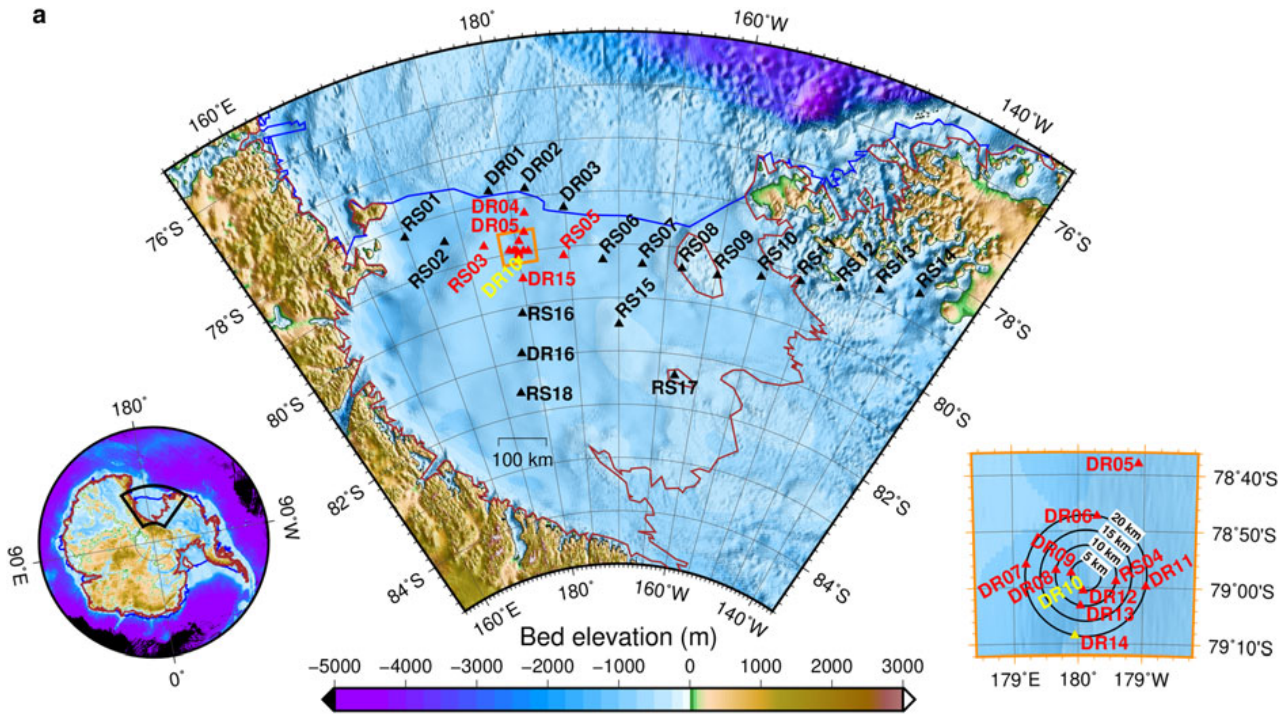
$W_1=200$, $W_2=300$ pixels
 $n=100$, $Q=200$, $T=1$

Fan-Chi Lin, Geophysics, 8mill Rays



Bianco 2018, 2019

Noise monitoring Ross Ice Shelf, Antarctica



Gravitational restoring force

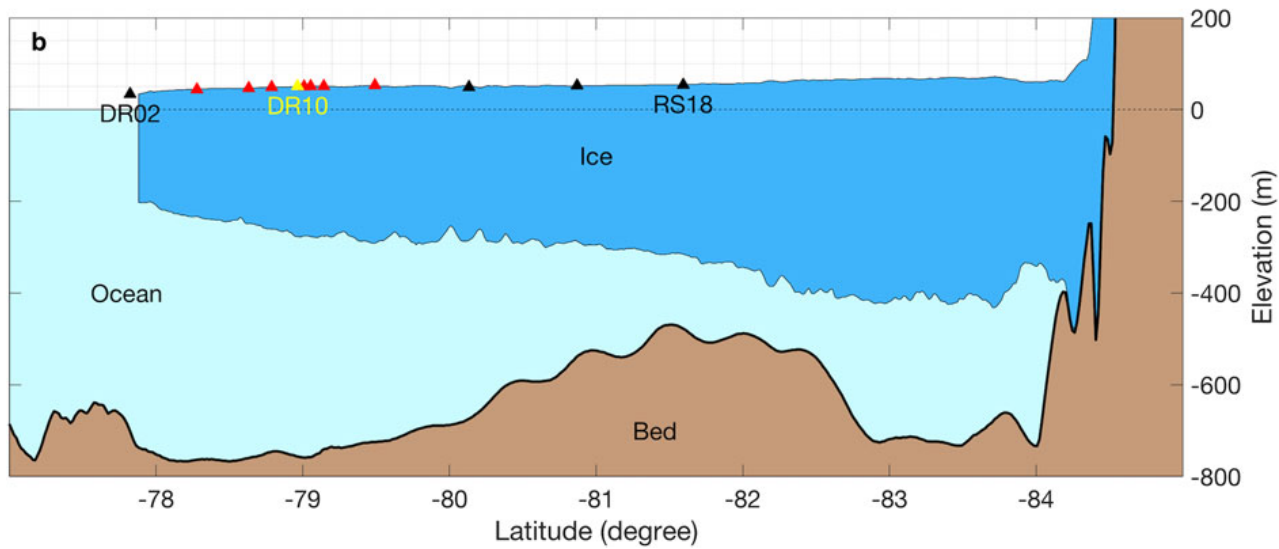
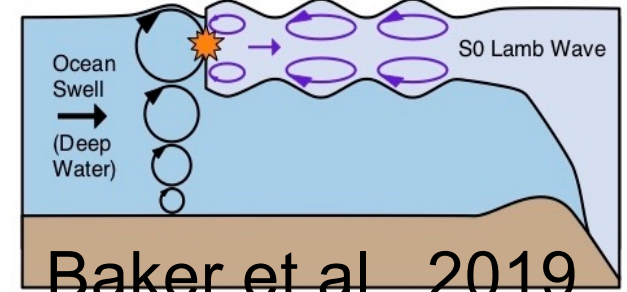
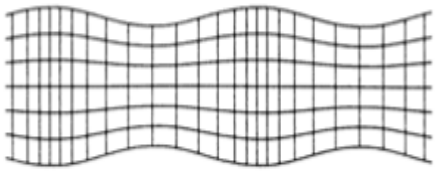
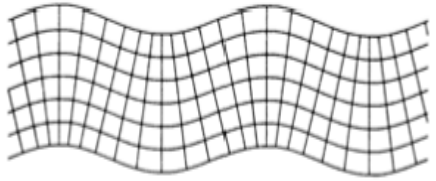


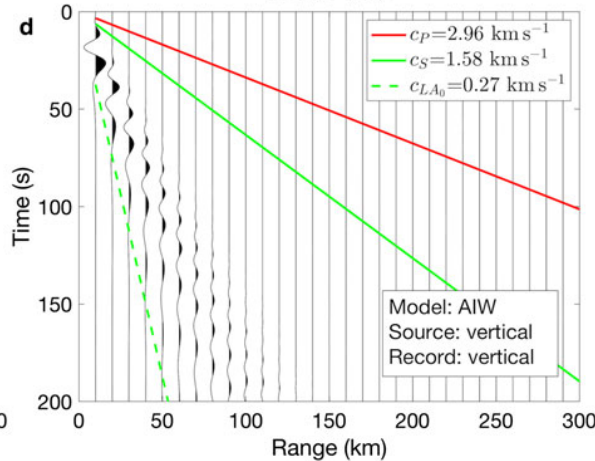
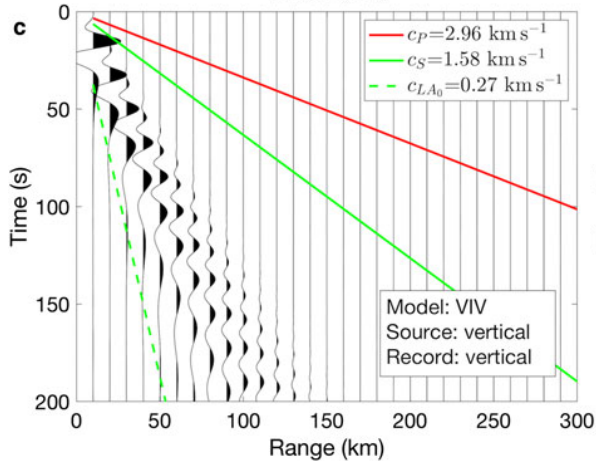
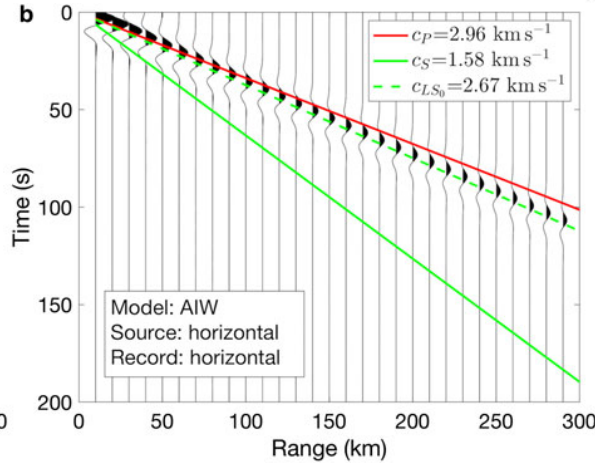
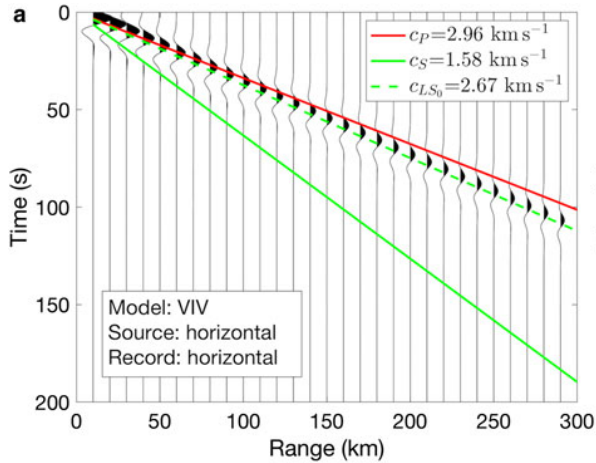
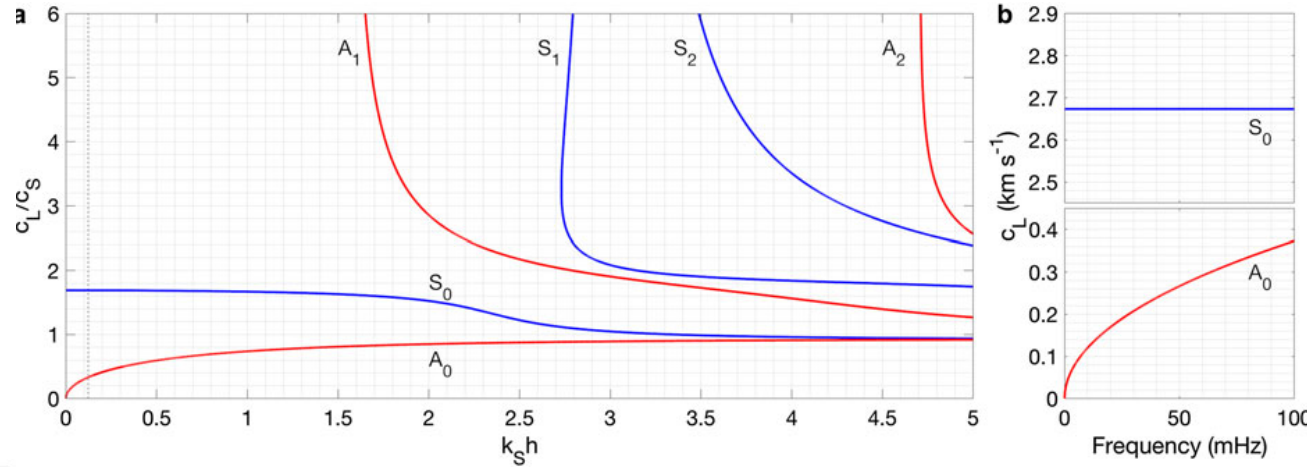
Plate waves simulated



Symmetric Lamb Wave

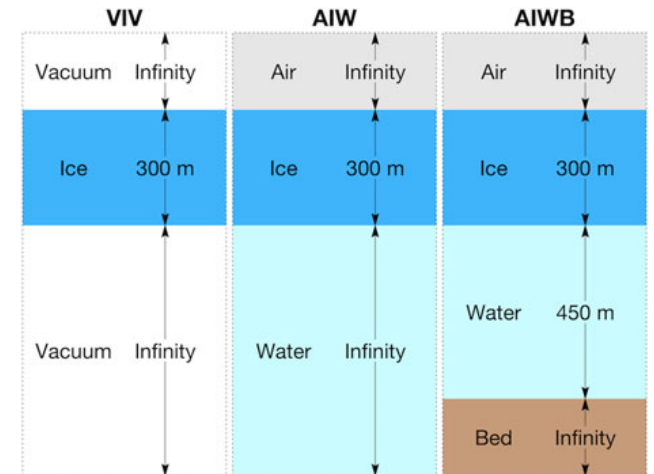


Anti-Symmetric Lamb Wave

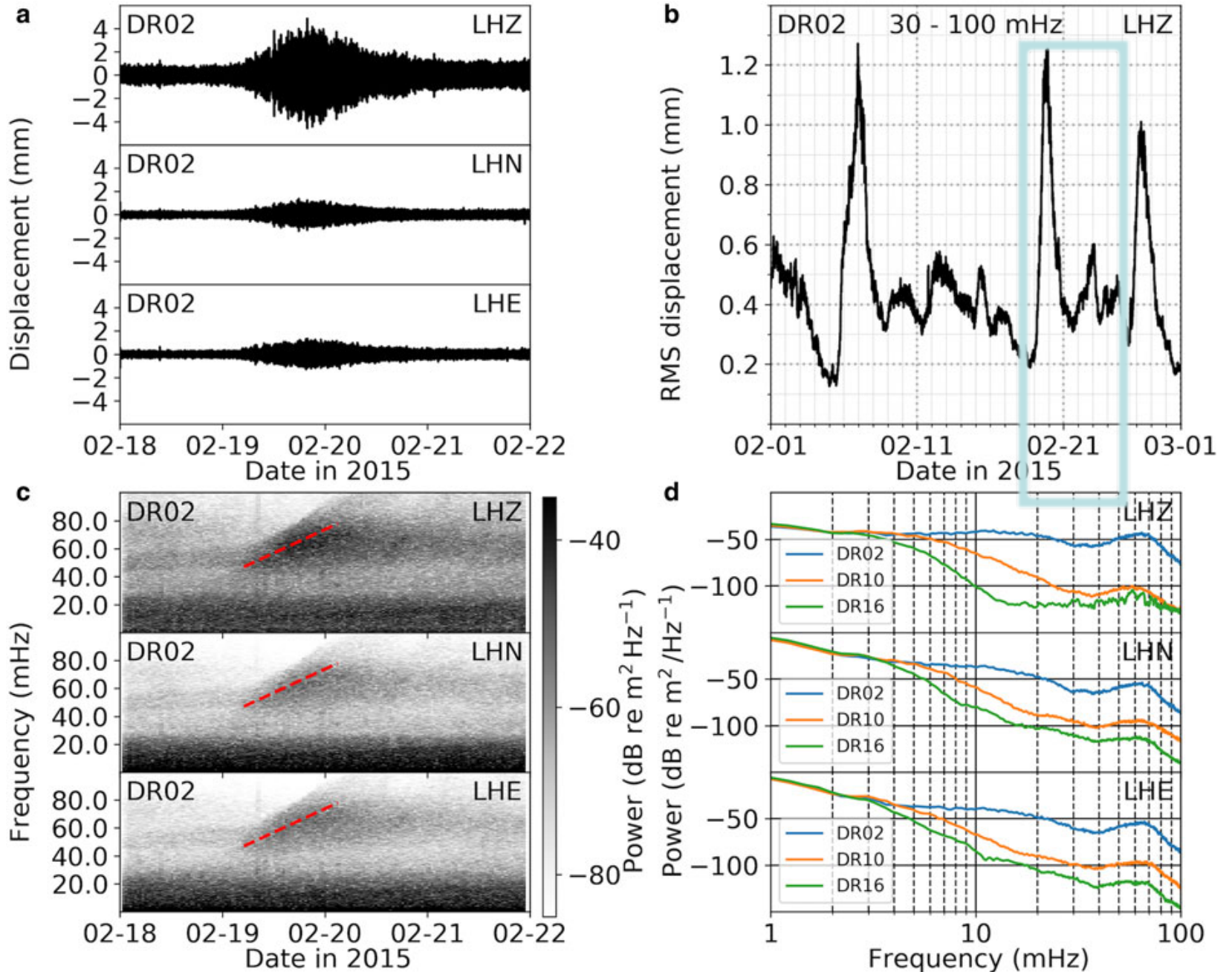


Iceplate 300m thick, $C_s=1.6\text{km/s}$

$$k_s h = \frac{2\pi f h}{c_L} = \frac{2\pi * 0.1 * 300}{1600} = 0.1$$

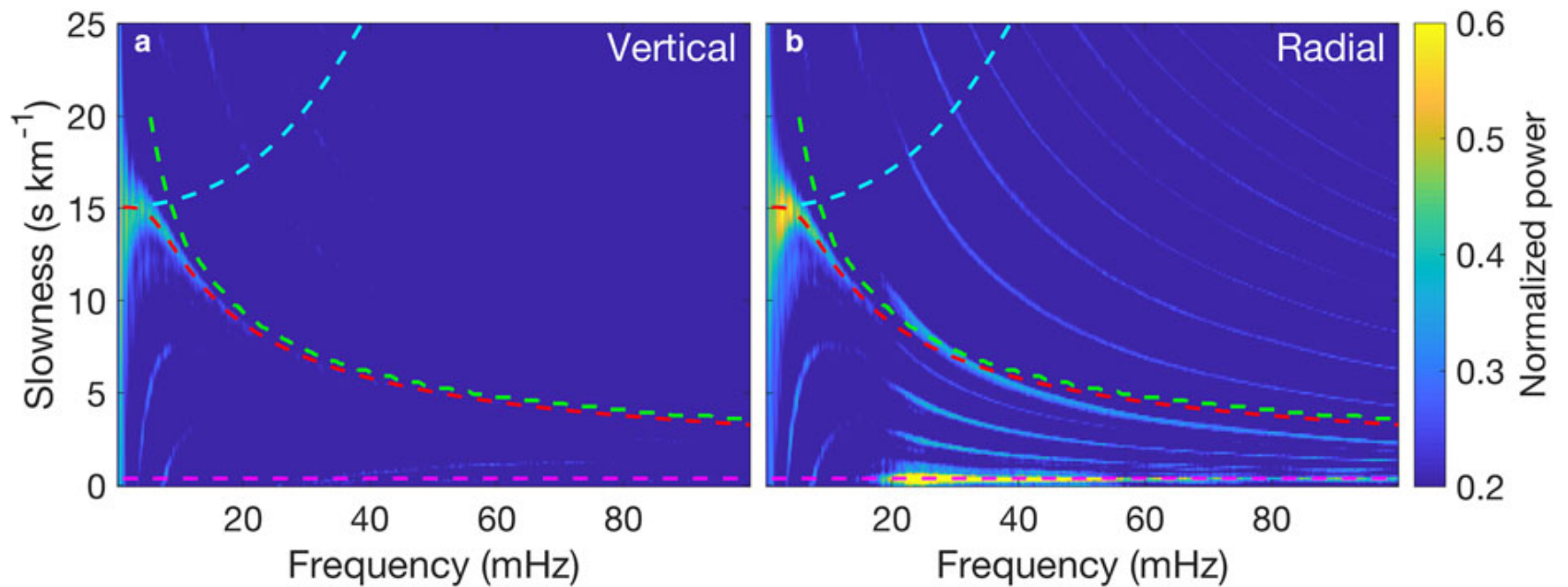


Strong IG event Feb 2015



Range to storm 2000 km.

Slowness spectra 19-21 Feb 2015



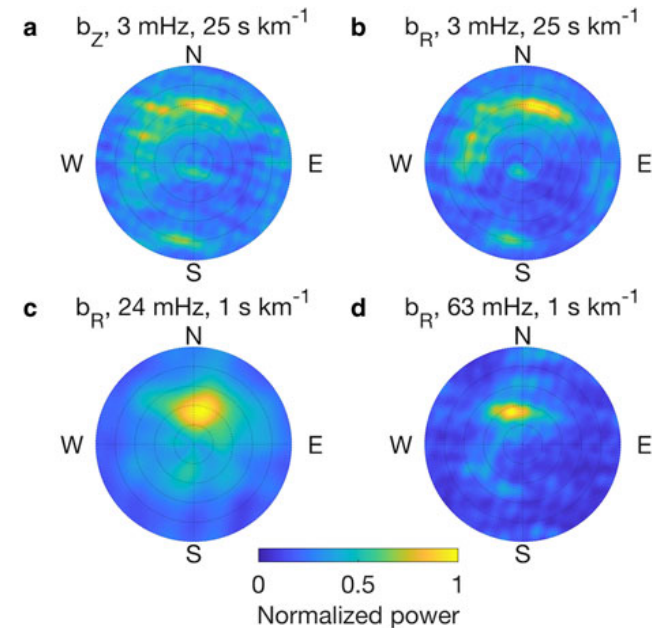
Obtained by averaging the beamforming output over 0- 20° azimuth. Phase speed dispersion curves of

ocean gravity waves,

flexural waves,

flexural-gravity waves

S_0 Symmetric AIWB model



Ambient seismic noise in the firn layer

AGU100 ADVANCING EARTH AND SPACE SCIENCE



Geophysical Research Letters

RESEARCH LETTER

10.1029/2018GL079665

Key Points:

- High-frequency (>5 Hz), narrow-band signals observed on an ice shelf are sensitive to changes in the near-surface firn layer
- Spectral peak frequency changes coincide with melt/freeze events on the ice shelf as well as with storm-driven redistribution snow
- Melt events have a unique spectral signature and can be modeled in terms of the penetration depth to which these thermal anomalies diffuse

Supporting Information:

- Supporting Information S1

Correspondence to:

J. Chaput,
jchaput82@gmail.com

Citation:

Chaput, J., Aster, R. C., McGrath, D., Baker, M., Anthony, R. E., Gerstoft, P., et al. (2018). Near-surface environmentally forced changes

Near-Surface Environmentally Forced Changes in the Ross Ice Shelf Observed With Ambient Seismic Noise

J. Chaput^{1,2}, R. C. Aster³, D. McGrath³, M. Baker³, R. E. Anthony⁴, P. Gerstoft⁵, P. Bromirski⁵, A. Nyblade⁶, R. A. Stephen⁷, D. A. Wiens⁸, S. B. Das⁷, and L. A. Stevens⁹

¹Department of Mathematics, Colorado State University, Fort Collins, CO, USA, ²Department of Geological Sciences, University of Texas at El Paso, El Paso, TX, USA, ³Department of Geosciences, Colorado State University, Fort Collins, CO, USA, ⁴U.S. Geological Survey, Albuquerque Seismological Laboratory, Albuquerque, NM, USA, ⁵Scripps Institution of Oceanography, University of California, San Diego, La Jolla, CA, USA, ⁶Department of Geosciences, Pennsylvania State University, State College, University Park, PA, USA, ⁷Woods Hole Oceanographic Institution, Woods Hole, MA, USA, ⁸Department of Earth and Planetary Sciences, St. Louis, MO, USA, ⁹Lamont-Doherty Earth Observatory, Columbia University, Palisades, NY, USA

Abstract Continuous seismic observations across the Ross Ice Shelf reveal ubiquitous ambient resonances at frequencies >5 Hz. These firn-trapped surface wave signals arise through wind and snow bedform interactions coupled with very low velocity structures. Progressive and long-term spectral changes are associated with surface snow redistribution by wind and with a January 2016 regional melt event. Modeling demonstrates high spectral sensitivity to near-surface (top several meters) elastic parameters. We propose that spectral peak changes arise from surface snow redistribution in wind events and to velocity drops reflecting snow lattice weakening near 0°C for the melt event. Percolation-related refrozen layers and layer thinning may also contribute to long-term spectral changes after the melt event. Single-station observations are inverted for elastic structure for multiple stations across the ice shelf. High-frequency ambient noise seismology presents opportunities for continuous assessment of near-surface ice shelf or other firn environments.

And then, late night TV...

EARTH SCIENCE

Scientists Discover a Weird Noise Coming From Antarctic Ice Shelf



Brian Kahn

10/16/18 4:52pm • Filed to: ICE ON THIN ICE

615.3K 84 6

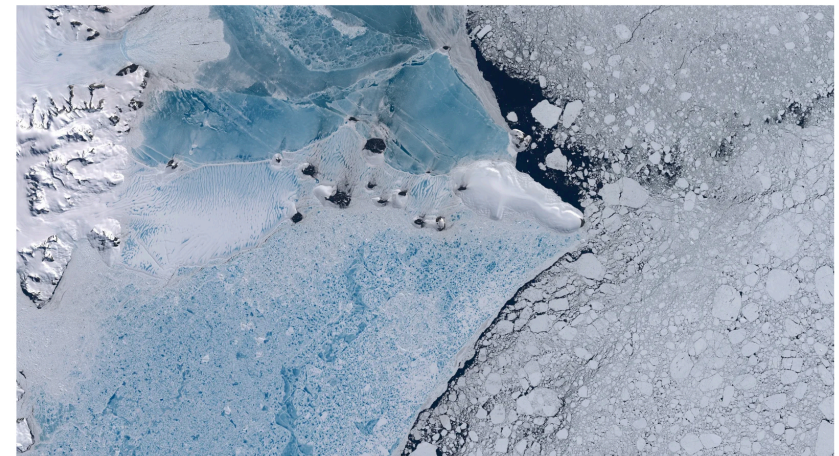
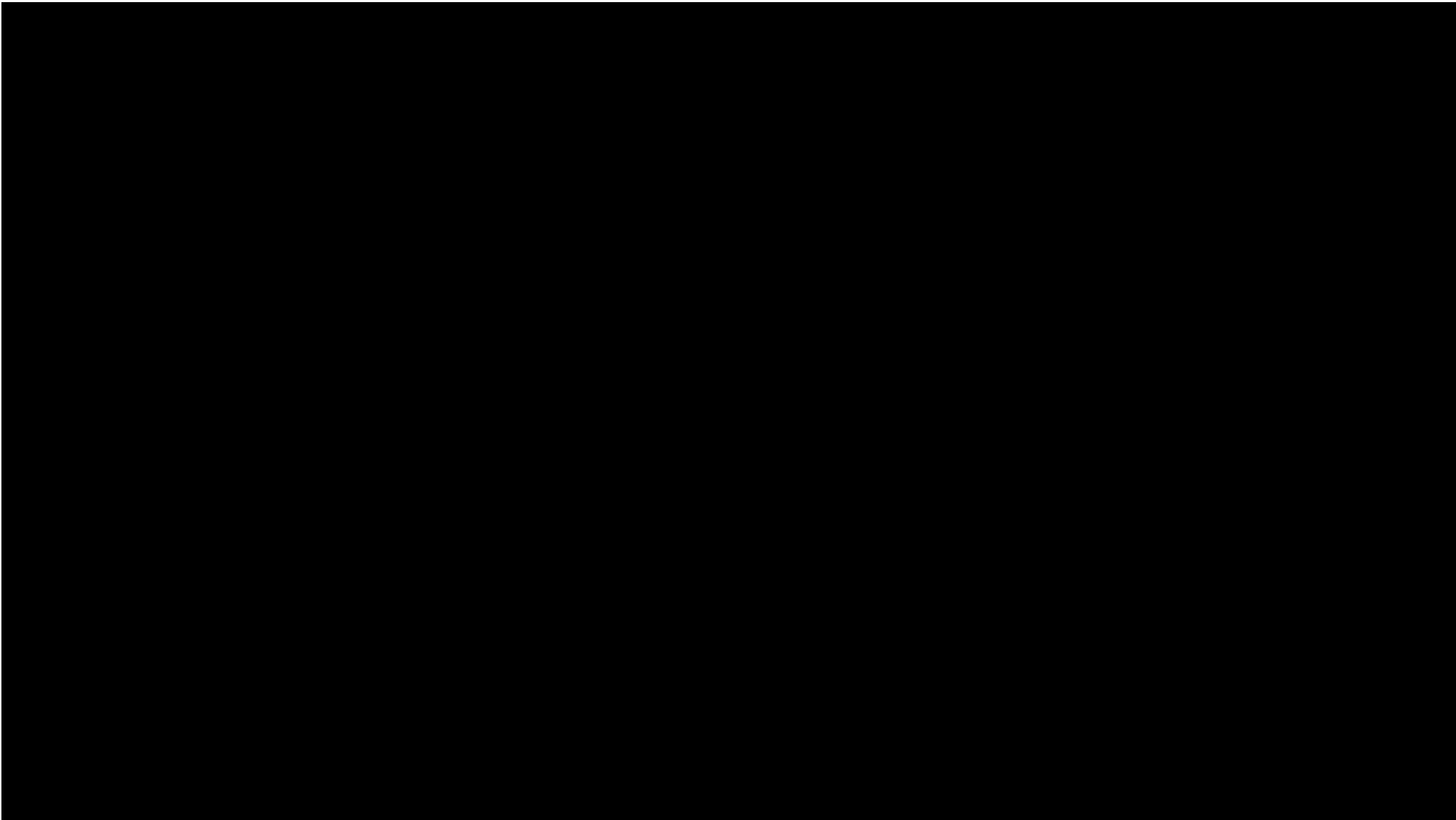


Photo: O.V.E.R.V.I.E.W. (Flickr)

The Antarctic is no stranger to weird sounds, from [ancient trapped air bubbles](#) popping to entire [ice sheets disintegrating](#). Now we can add another freaky track to the oeuvre of icy masterpieces.



FINITO

